OCS Study
MMS 94-0053

University Research Initiative

Satellite-Based Assessment of the Mississippi River Discharge Plume's Spatial Structure and Temporal Variability

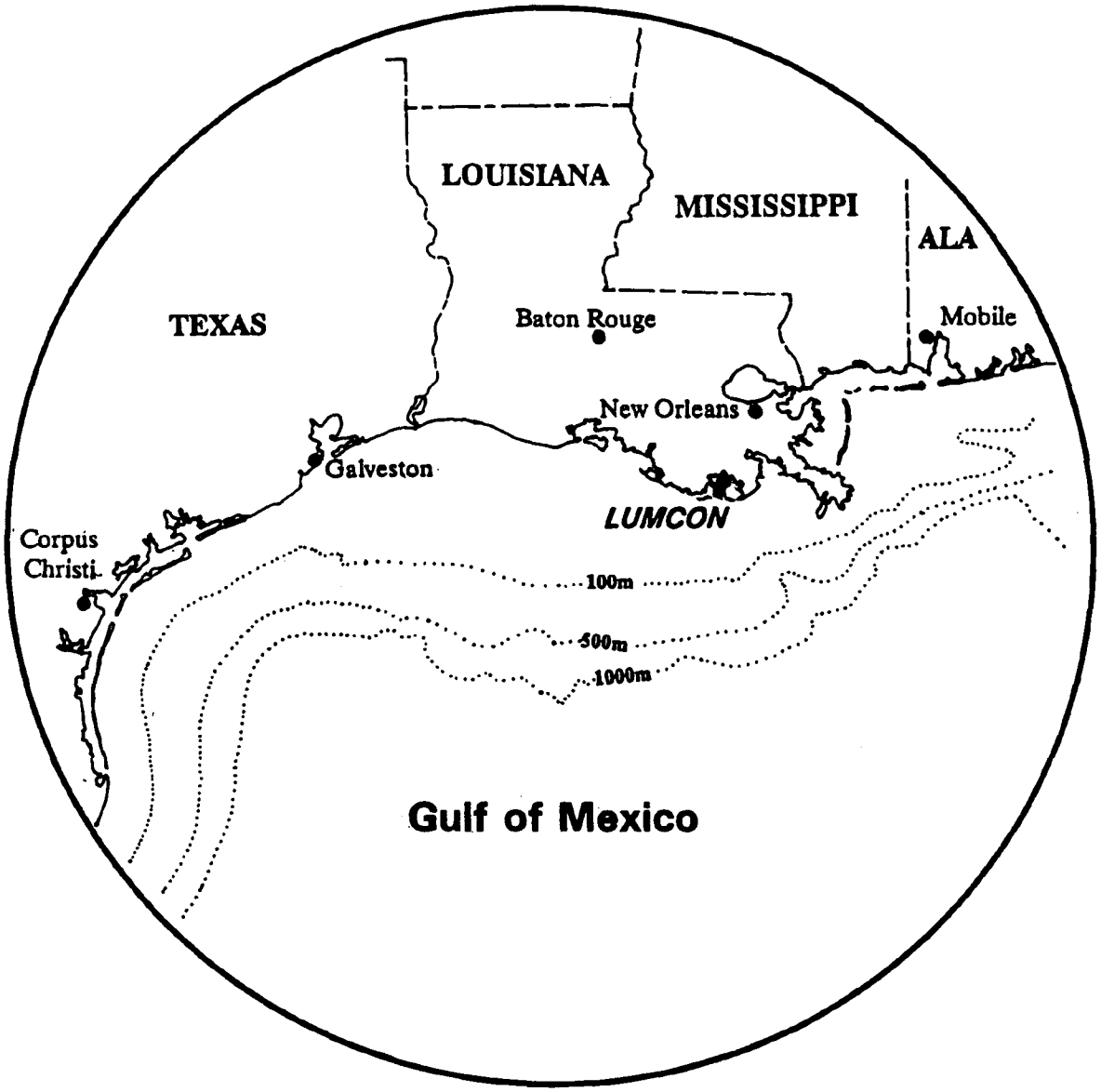

MMS U.S. Department of the Interior
Minerals Management Service
Gulf of Mexico OCS Region

LUMCON Cooperative Agreement
University Research Initiative
Louisiana Universities Marine Consortium

OCS Study
MMS 94-0053

University Research Initiative

Satellite-Based Assessment of the Mississippi River Discharge Plume's Spatial Structure and Temporal Variability

Author

Nan D. Walker
Coastal Studies Institute
Louisiana State University
Baton Rouge, Louisiana

November 1994

Prepared under MMS Contract
14-35-0001-30470
by
Louisiana Universities Marine Consortium
8124 Highway 56
Chauvin, Louisiana 70344

Published by

U.S. Department of the Interior
Minerals Management Service
Gulf of Mexico OCS Region

Cooperative Agreement
University Research Initiative
Louisiana Universities Marine Consortium

DISCLAIMER

This report was prepared under contract between the Minerals Management Service (MMS) and the Coastal Studies Institutes, Louisiana State University. This report has been technically reviewed by the MMS and approved for publication. Approval does not signify that the contents necessarily reflect the views and policies of the Service, nor does mention of trade names or commercial products constitute endorsement or recommendation for use. It is, however, exempt from review and compliance with MMS editorial standards.

REPORT AVAILABILITY

Extra copies of the report may be obtained from the Public Information Unit (Mail Stop 5034) at the following address:

U.S. Department of the Interior
Minerals Management Service
Gulf of Mexico OCS Region
Public Information Unit (MS 5034)
1201 Elmwood Park Boulevard
New Orleans, Louisiana 70123-2394
Telephone Number: 1-800-200-GULF

CITATION

Walker, N.D. 1994. Satellite-based assessment of the Mississippi River discharge plume's spatial structure and temporal variability. OCS Study MMS 94-0053. U.S. Dept. of the Interior, Minerals Management Service, Gulf of Mexico OCS Region, New Orleans, La., 56 pp.

ABSTRACT

The Mississippi River is the major contributor of sediments, pollutants, and nutrients to the northern Gulf of Mexico. This study utilized five years of NOAA Advanced Very High Resolution Radiometer (AVHRR) satellite data (1989-1994) to investigate the spatial and temporal variabilities of the sediment plume and to enable the determination of which environmental forcing factors affect plume dispersal.

Annual and interannual variability in plume area occurs in association with large changes in river discharge. In 1989, during spring high river discharge (March/April), the Mississippi River plume averaged 4595 km^2, whereas during autumn low river discharge (October) the plume averaged 2058 km^2. The interannual variability of the plume during spring was found to be similar in magnitude to the annual variability. During spring, average plume areas ranged from a low of 1836 km^2 in 1992 under medium discharge conditions to a high of 4592 km^2 in 1989 under high discharge conditions. Although the time-averaged plume was clearly related to large variations in river discharge, tremendous day-to-day variability was observed which was unrelated to discharge.

Correlation and multiple regression techniques were used to identify the most important environmental variables affecting plume variability and to quantify these relationships for possible predictive applications. Wind forcing was identified as the most important environmental variable, after river discharge. The east, south, and west plume parameters were maximized by winds from different directions. West of the delta, plume area increased during episodes of eastward winds. During winter, southward winds increased the western plume area as well as the western extent of the sediment plume. Northward and eastward winds increased the size and extent of the plume east of the delta. The offshore extent of the plume was maximized by eastward winds.

The plume parameters best predicted by the multiple regression models were plume area, east and west of the delta. The best predictive model for the western area was obtained from May through September when 64% of plume variability was explained by river discharge, wind speed, and the east-west wind component. The best model for the eastern plume area was obtained from May through September when river discharge, the north-south and east-west wind components explained 70% of plume variability. An extreme river circulation event occurred in late July and August 1993, during the Great Flood of 1993, which exemplifies the relationship between northeastward wind forcing and the eastward dispersal of Mississippi plume waters.

TABLE OF CONTENTS

LIST OF FIGURES

LIST OF TABLES

ACKNOWLEDGEMENTS

Many thanks are extended to Dr. Oscar Huh, Director of the Earth Scan Lab (ESL), and Dr. Lawrence Rouse, Associate Director of the ESL, for establishing the historic data archive used in this study. Dr. Lawrence Rouse is also thanked for assisting in data processing. Gratitude is extended to David Wilensky, Systems Manager of the ESL, for software development. The undergraduate staff of the ESL is acknowledged for their invaluable assistance in image processing. Colin Murray is heartily thanked for his able assistance in performing the statistical analyses. Celia Harrod is thanked for assisting in figure preparation. Last, but certainly not least, Debra Milam and April Hawkins are gratefully acknowledged for typing this manuscript.

INTRODUCTION

The Mississippi River is the major source of fresh water, sediments, nutrients and pollutants for the Gulf of Mexico. Draining 41% of the continental U.S., it discharges freshwater into the northern Gulf of Mexico through the bird-foot delta region at an average rate of 14,000 m^3s^{-1} Mossa (1990) and, in addition, transports about 150 million tons of sediment to the Gulf annually (Milliman and Meade 1983). The Atchafalaya River (the major distributary of the Mississippi River) carries approximately one-half of this amount. Although the Mississippi River is the largest river in North America and 6th largest worldwide in terms of discharge (Milliman and Meade, 1983) few studies have focused on the fate of river water once it enters the Gulf of Mexico.

Satellite-acquired data can provide valuable information on the distribution of river water and sediments on the continental shelf as well as on the circulation processes affecting the fate of riverborne sediments and pollutants. This type of data yields synoptic coverage over large geographic areas, unattainable from research ships or moorings. Numerous investigators have utilized satellite data as the primary data source in studying river systems, estuaries and the interaction of river plumes with oceanic water (Rouse and Coleman 1976, Gagliardini et al. 1984, Schroeder et al. 1985, Stumpf 1988, Muller-Karger et al. 1988, Dinnel et al. 1990).

This Mississippi River sediment plume is easily detected using reflectance information obtained by the Advanced Very High Resolution Radiometer of the NOAA Satellites. The river water can also be detected using thermal infrared satellite data when river water temperatures contrast with those of the continental shelf. A knowledge of the spatial distribution and circulation characteristics of plume waters is of utmost importance to the understanding of hypoxia and the distribution of pollutants in the northern Gulf of Mexico. This study has been based on the analysis and interpretation of data obtained by the Advanced Very High Resolution Radiometer (AVHRR) aboard the National Oceanographic and Atmospheric Administration (NOAA) series of environmental satellites from 1989 through 1993.

The primary objectives of this study were:

1. to determine quantitatively which areas of the continental shelf are most influenced by riverborne sediments, pollutants, and nutrients by examining the Mississippi River's discharge plume with 5 years of synoptic digital satellite data obtained by the Advanced Very High Resolution Radiometer (AVHRR) of the NOAA environmental satellites.

2. to assess the relationships between the morphology of the Mississippi River discharge plume and environmental forcing parameters including river discharge, local wind forcing (on various time-scales), tidal range and phase and shelf/slope current phenomenon (such as Loop Current intrusions).

With the exception of the pioneering work of Rouse and Coleman (1976) using LANDSAT data, no satellite study of this type has focused on the Mississippi River plume region. Therefore, this study should provide important baseline information of use to environmental managers and researchers in wide-ranging fields of oceanography and hydrology.

BACKGROUND INFORMATION

The Mississippi River discharges into the northern Gulf of Mexico through the Balize (bird-foot) and Atchafalaya delta regions (Figure 1). Flow down the Atchafalaya River is limited to 30% of the total Mississippi River flow by the Old River Control Structure. The total annual discharge of the Mississippi/Atchafalaya River system is 507 km^3 which amounts to 10% of the volume of the entire Louisiana-Texas shelf out to the 90 meter bathymetric contour (Dinnel and Wiseman 1986, Dagg and Whitledge 1991). The freshwater influence from these rivers has been observed as far as Port Aransas, Texas, a distance of 800 km from the Mississippi River Balize delta (Smith 1980).

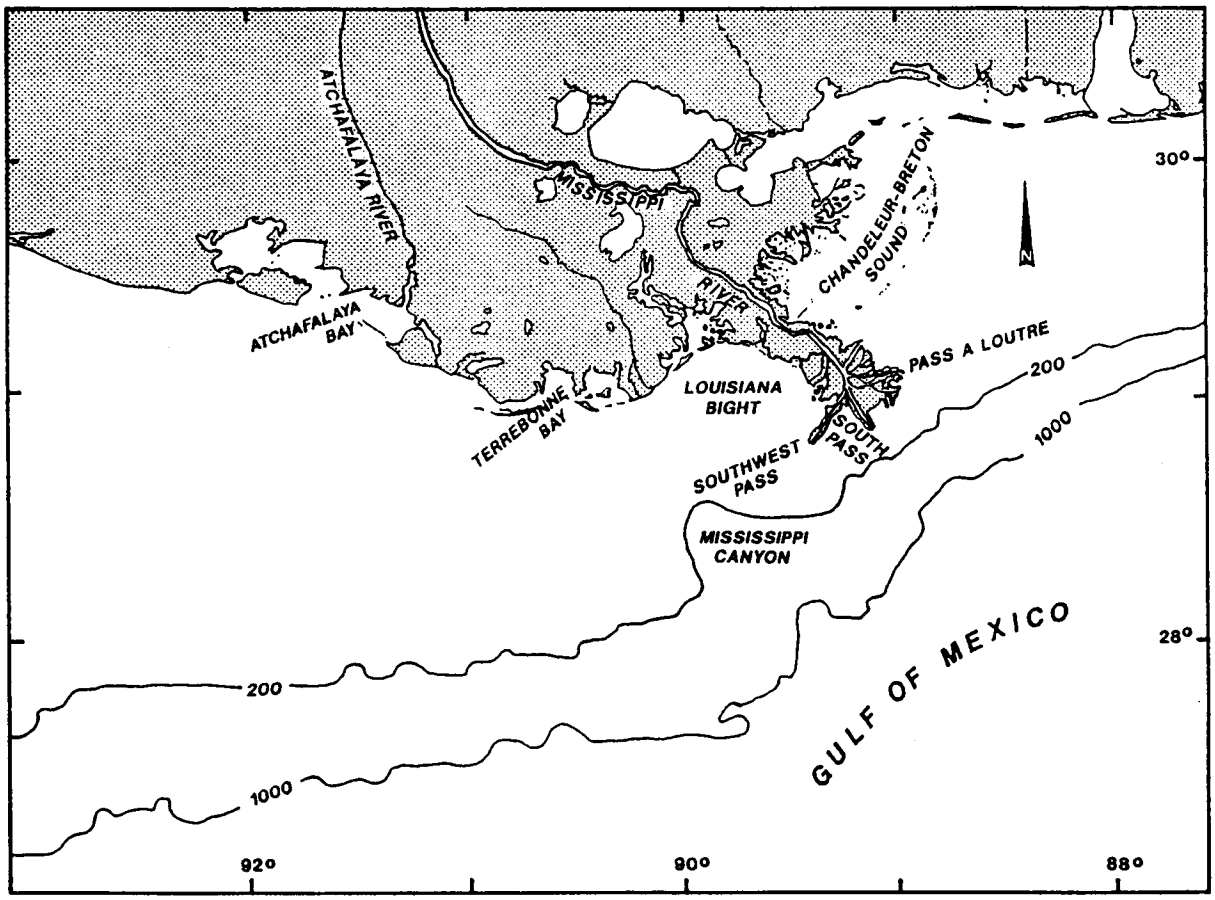

Figure 1. Map of the main study area. Contours are in meters.

The inputs of freshwater, sediment, nutrients, and pollutants have a major impact on all aspects of continental shelf oceanography in the northern Gulf of Mexico. The input of nutrients ensures that the region surrounding the Mississippi River delta is highly productive in terms of phytoplankton and zooplankton production (Dagg et al. 1987, Lohrenz et al. 1990). Research results of Walsh et al. (1989) suggest that the Mississippi plume area is the most productive within the Gulf of Mexico. The entire Louisiana/Texas shelf supports a very productive fishery which amounts to 28% of the total U.S. catch (Rabalais et al. 1991) and spawning of key species, such as Gulf menhaden (Brevortia patronus), is concentrated around the Mississippi Delta (Sogard et al. 1987). There are negative consequences of the high productivity in that a large zone of hypoxia is generated during summer months over much of the Louisiana continental shelf west of the Balize delta (Rabalais et al. 1991). In addition to the nutrient input, the fine-grained river sediments in suspension carry an abundance of pollutants, which are potentially dangerous to fish and shellfish (Jay Means, Professor, Environmental Chemistry and Toxicology, Louisiana State University, personal communication). Approximately 90% of sediment within the river is transported as suspended load (Fisk et al. 1954); of which, 40% typically consists of silt, 50% of clay and 10% of very fine sand (Wright and Coleman 1974). Sediment is an important resource to Louisiana, the state which is experiencing the highest land loss rates in the United States. Results of this study will provide important information concerning the distribution of sediment on the continental shelf which should enable more effective management of Mississippi River sediments.

This study concentrates on the fate of the Mississippi River discharge through the Balize delta region, which includes approximately 70% of the entire flow. South of Venice, at Head of Passes, the Mississippi River branches into three major distributaries: Southwest Pass, South Pass, and Pass a Loutre. The percentage flow through these main distributaries has been estimated at 30%, 15%, and 30% , respectively (U.S. Army Corps of Engineers 1984). The remaining 25% is discharged through secondary channels.

At the mouths of the passes, the river experiences buoyant expansion and mixing due to wave, wind and tidal currents on the continental shelf (Wright and Coleman 1974). The freshwater "plume" produces a halocline within the upper 10 meters even when cold water overlies warm (Wiseman and Dinnel 1988). The thickness of the freshwater "lens" which overlies more saline ambient Gulf water increases with increasing river discharge and under the presence of wave-induced mixing (Wright 1970). Stratification of the water column generally increases with increasing discharge (usually in spring) and in association with weak winds of summer (Rabalais et al. 1991). Strong thermal and color fronts are often observed on the south and east sides of the Balize delta region as a result of convergence of river water with ambient Gulf water (Wright and Coleman 1974). Wright and Coleman (1971) found a band of shelf water of intermediate salinity between the river water and ambient Gulf water which they suggested originated from passes to the northeast of South Pass.

Circulation on the inner continental shelf near the Balize delta is primarily wind-driven (Murray 1972, Schroeder et al. 1987). The prevailing winds offshore of the delta are easterly; southeasterly from March through September and northeasterly from October through February (Rhodes et al. 1985). Thus, the wind-driven surface currents are primarily westward. In addition, the nearshore pressure gradient set up by river runoff drives a westward geostrophic flow near the coast (Schroeder et al. 1987) which enhances the wind-induced westward current.

From October through March, cold front passages perturb the prevailing easterly wind regime. They occur every 3 to 10 days (Fernandez-Partegas and Mooers 1975) and are characterized by a clockwise rotation in the wind field; from southeast to southwest, northwest, and northeast. Strongest winds usually blow from the northerly quadrants. Winds associated with cold-front passages have important effects on shelf circulation (Huh et al. 1978, Schroeder et al. 1987, Wiseman and Dinnel 1988). In addition, Loop Current filaments and eddies can affect circulation in the vicinity of the Balize delta (Wiseman and Dinnel 1988, Ebbesmeyer et al. 1982). Shelf currents in excess of 2 ms^{-1} have been caused by the intrusion of Loop Current filaments onto the shelf and slope where they have seriously disrupted oil and gas activities in the northern Gulf of Mexico (Huh and Schaudt 1990).

The Balize delta extends nearly completely across the Mississippi/Louisiana continental shelf, essentially blocking the shelf to significant amounts of east-west flow (Wiseman and Dinnel 1988). Chew et al. (1962) suggest that a saddle point in the general Gulf circulation exists in front of the delta, with eastward flow occurring along the shelf edge east of the delta and westward flow occurring west of the delta. Schroeder et al. (1987) concur with the suggestion of Chew et al. (1962) and also report the existence of anti-clockwise circulation on the shelf east of the delta with westward flow along the inner shelf in approximately 20-30 meters of water. Also in agreement with Chew et al. (1962), Cochrane and Kelly (1986) and Wiseman et al. (1976) report westward outer shelf flow west of the delta. On the inner shelf west of the delta, in the Louisiana Bight, a clockwise circulation has been previously reported (Wiseman et al. 1976, Rouse and Coleman 1976). Little is known about the mean surface drift directly south of the delta (Wiseman and Dinnel 1988).

Wright (1970) suggested that the tidal regime plays an important role in circulation at the mouth of South Pass. He found that the South Pass discharge "plume" turned more abruptly westward during flooding tide since the flood tidal wave travels from east to west. Generally, however, tidal currents are relatively weak in this region averaging about 15 cms^{-1} (Murray 1972). Tides in the area are mainly diurnal and have an average range of 30 cm (Murray 1972). Semidiurnal effects appear in the tide only during times of equatorial tides when tidal currents are weakest.

METHODOLOGY

Satellite Data Overview

This study utilizes digital data acquired by the Advanced Very High Resolution Radiometer (AVHRR) of the NOAA environmental satellites. This satellite data type was chosen as the main data source for several reasons. It provides the best available temporal resolution, at least 4 scenes/day, which enables assessments of daily changes in plume morphology, under clear-sky conditions. The spatial resolution (1.1 km) and regional coverage are optimal for studying the surface morphology of the river plume and simultaneous circulation features seaward of the river mouths. These data have been archived daily since July 1988 by the Coastal Studies Institute's Earth Scan Laboratory. The AVHRR provides five channels of information, two in the visible (yielding information on suspended sediment concentrations) and three in the thermal infrared range (for computing sea surface temperatures). Table 1 shows the wavelength characteristics of these five channels.

Table 1. NOAA Advanced Very High Resolution Radiometer (AVHRR) Characteristics.

Channel	Wavelength (μm)	Spatial Resolution (km)	Swath Width (km)
1	0.58 - 0.68	1.1	2800
2	0.70 - 1.1	1.1	2800
3	3.5 - 3.9	1.1	2800
4	10.5 - 11.5	1.1	2800
5	11.5 - 12.5	1.1	2800

As this is the first comprehensive study of the Mississippi River plume using satellite data, a large geographic area was included in the analysis: 25^0 to 31^0 N latitude and 86^0 to 98^0 W longitude.

The Mississippi River plume is revealed very differently by the visible (reflectance) and thermal infrared (SST) channels. Reflectance information provides a quantitative means of defining the Mississippi River sediment plume, and, therefore, has been used as the primary source of information in this report. The main drawback to its use is that once the suspended sediment has dropped out of suspension, the plume is no longer detectable by the satellite sensor. In terms of SST, the plume is "trackable" if the temperature of Mississippi River water is substantially different from that on the continental shelf. This is often the case during autumn and spring when river water is generally cooler than the ambient shelf waters, as it has originated further north. During mid-winter, however, the shelf waters are often of a similar temperature to Mississippi River water, making it more difficult to track river water on the

shelf. The SST signal, however, can be very useful in defining the maximum spatial extent of the Mississippi River plume, and it has been used for that purpose in this study. The SST information is also useful for detecting water of Loop Current origin. Its usefulness, however, deteriorates in summer due to high atmospheric water vapor loads and weak or non-existent SST gradients on the shelf.

Satellite Data Processing

The visible channels of the AVHRR, when properly processed, can provide important information on surface suspended sediment distribution and variability. The sediment plume also provides information concerning the distribution of pollutants in the northern Gulf of Mexico, as many pollutants are carried on fine-grained river sediments. It is desirable to be able to relate the satellite radiance information to in-situ concentrations of suspended sediments and, for this reason, a field component was included in Year 1 of this project (Walker and Rouse, 1983). The reader is referred to the Year 1 report for a description of this field program.

In order to make comparisons of suspended sediment concentrations from image to image, it is necessary to perform certain atmospheric corrections to the satellite data to obtain water reflectances. The bias technique of Stumpf (1988, 1992) was implemented within the Terascan™ image processing software. A summary of the bias correction method is given below.

Water reflectance requires a correction for Rayleigh scattering, for aerosols, for the elevation of the sun, and for some transmission losses. The Rayleigh component does not change rapidly in the red and near infrared parts of the spectrum. Thus, when working in areas on the order of 200 km in the east-west direction, the Rayleigh component can be treated as a bias, simplifying the computation. Using this method, the water column reflectance R_d can be found from:

$R_d \approx R_d' = R_c - R_{bias}$

where:

$$R_c = \left[\frac{A(1)}{T_0(1)T_1(1)} - \frac{A(2)}{T_0(2)T_1(2)} \right] \qquad (1/r^2) * (1 / \cos \Theta)$$

$A(\lambda)$ = albedo for channel λ, where $A = G * C + I$; G and I are calibration coefficients, and C = count value (0 - 1023)

$T_0(\lambda) = \exp [-(t_r(\lambda) / 2 + t_o(\lambda)) / \cos \Theta]$
$T_1(\lambda) = \exp [-t_r(\lambda) / 2 + t_o(\lambda)]$

$(1/r^2) = [1 + 0.0167 \cos j]^2$ and $j = 2\pi (D - 3) / 365$; D is the Julian day

$\cos \Theta$ = cosine of solar zenith angle at scene center
$t_r(\lambda)$ = Rayleigh optical depth for channel
$t_o(\lambda)$ = ozone and water vapor absorption optical depth for channel

and R_{bias} is the residual reflectance defined as R_c for a clear atmosphere over clear water near the area of interest.

For turbid water, reflectance can be approximated by the equation:

$R_d' = (y * F) / (1 + G/n)$

where n is the suspended sediment concentration in mgl^{-1}, y is 0.178, and

$F = b^* / (b^* + a^*)$ where b^* is the specific backscatter coefficient for sediment and a^* is the absorption coefficient for sediment

$G = a_x / (b^* + a^*)$ where a_x is the absorption coefficient for non-sediment constituents.

From Stumpf (1988, 1992).

The equation was solved with the Newton method of non-linear curve-fitting using the suspended sediment concentrations obtained from the field sample analysis for 'n' and the satellite-derived reflectance values for 'R_d'. Figure 2 depicts the data points used to establish values for F and G in this study, the best-fit line and the 95% confidence limits. The root mean square error for this equation is 0.006. The coefficients obtained for the Mississippi River plume are similar to those obtained by Stumpf (1992) for Delaware Bay and Mobile Bay (Table 2).

Table 2. Coefficient comparisons.

Location	Satellite	F	G
Mississippi Plume (this study)	N-11	0.35	30.3
Delaware Bay (Stumpf 1992)	N-9	0.24	26.4
Mobile Bay (Stumpf 1992)	N-10/11	0.41	21.0

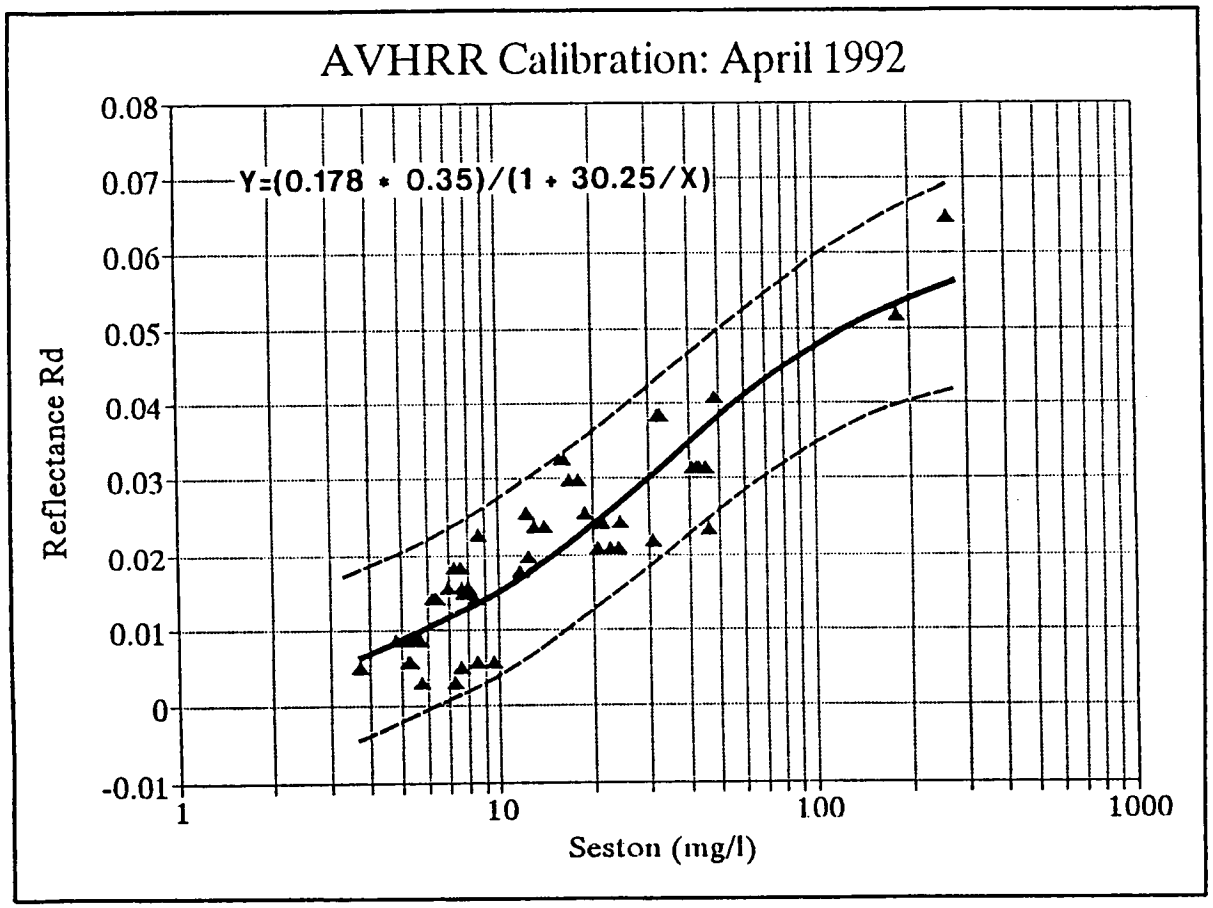

Figure 2. Suspended sediment concentration/AVHRR reflectance scatterplot and non-linear best fit equation.

Daytime data obtained by the NOAA-11 satellite were used to investigate suspended sediment distribution. This satellite has been operational since mid-October 1988 and passes over the northern Gulf of Mexico about 2100 GMT (1500 CST) and 0900 GMT (0300 CST). In contrast to NOAA-9 and NOAA-10 which suffered from serious degradation of the visible sensors, NOAA-11 has shown near zero drift since launch (Y.J. Kaufman, NASA Goddard Space Flight Center, personal communication). The decision to restrict the sediment analysis to NOAA-11 data enabled a quantitative investigation into the distribution and variability of the Mississippi River sediment plume. Since the thermal infrared data is calibrated underway, it does not suffer from sensor degradation problems. The analysis of sea surface temperature patterns was, therefore, not constrained to one satellite.

In Year 1 of this project at least two satellite images per day were uploaded from tape, calibrated and screened for cloud-cover during the time period from July 1988 through October 1992, yielding a total of 3000 images. Initially, cloud cover information from coastal weather stations was used in an attempt to reduce the amount of image processing to be performed. However, we found that the available coastal information did not adequately reflect cloud conditions over the northern Gulf of Mexico. Therefore, imagery was viewed for each day of the 4-year period. Satellite images of the Mississippi River plume or the northern Gulf of Mexico with less than 20% cloud-cover were saved for further processing. The additional processing steps included atmospheric correction for the retrieval of reflectance, calculation of SST, navigation and registration to a standard rectangular map projection. Sea surface temperatures were computed using the split-window multi-channel SST equations (McClain et al. 1985). The bias correction technique of Stumpf (1988, 1992) was used for the determination of reflectance. The processed satellite scenes were stored on 4 mm tapes for further screening by the principal investigator. During Year 2, satellite imagery obtained from January to September 1993 were added to the data base. The satellite data processing procedures are summarized in Figure 3.

The final satellite image data base used in the statistical analysis was comprised of 113 images (Table 3). Each image was processed as described above. The sediment plume was defined as areas where concentration exceeded 10 $mg \cdot l^{-1}$ using the calibration equation shown in Figure 2. Five measurements of the plume were used in the statistical analysis. The plume region was divided into an eastern and western area with a dividing line emanating from South Pass towards the southeast. The plume areas east and west of this line were digitized and called area west (AW) and area east (AE). In addition, three measurements were made documenting the distance of the plume from the delta; distance west (DW), distance east (DE) and distance south (DS). These measurements recorded the westernmost extent, the easternmost extent and the southernmost extent of the Mississippi River turbidity plume for each image. In the case of distance west, a meridian was drawn tangent to the western edge of the plume. Then a line was extended due west from Southwest Pass until it intersected this meridian. In the case of distance south, a line of latitude was drawn tangent to the southernmost extent of the plume. Then a north-south line was extended from Southwest Pass until it intersected this line of latitude. For distance east, a meridian was drawn tangent to the easternmost margin of the plume. Then a line was extended from the mouth of Pass a Loutre due east until it intersected the north-south meridian.

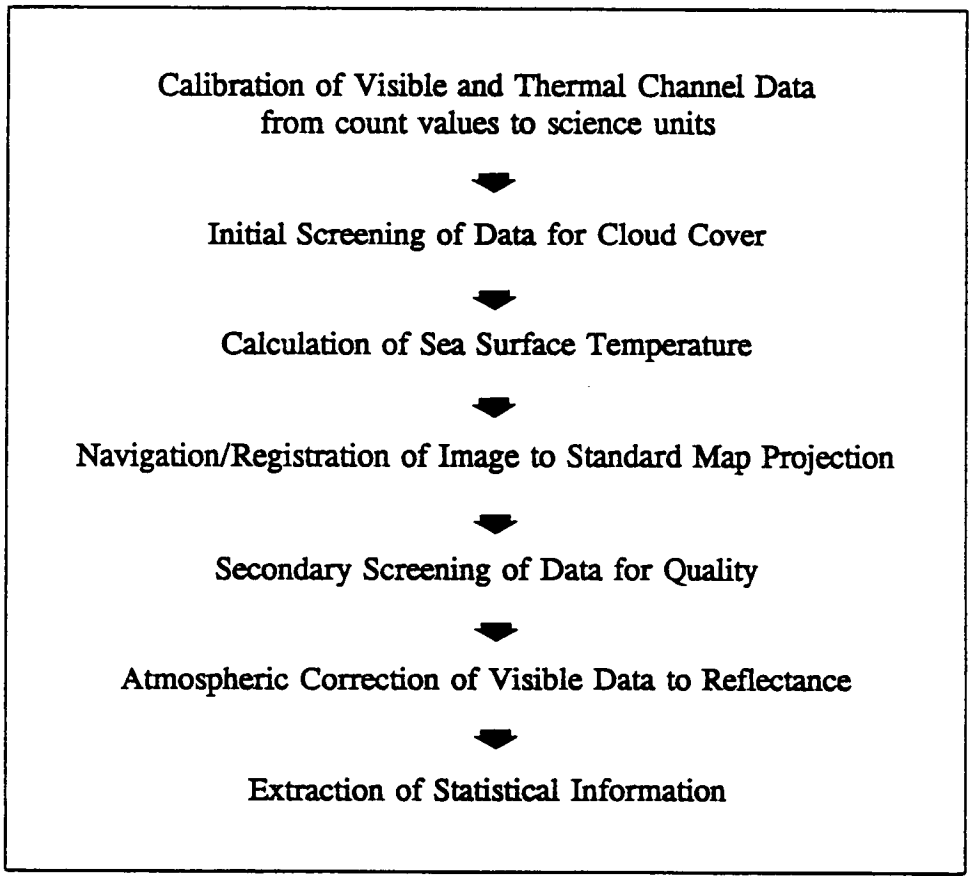

Figure 3. Summary of satellite data processing steps.

Table 3. Satellite image data base summary

Month	Year	Images/Month	Discharge ($m^3 \cdot s^{-1}$)	Average Plume Area		
				West	East	Total
Mar	1989	5	31088	2987	2631	5618
Apr	1989	6	25642	1695	1664	3359
Oct	1989	12	9128	880	1128	2008
Jan	1990	8	9656	1846	1323	3169
Mar	1990	5	26787	2749	1714	4463
Apr	1990	5	24691	1829	1538	3367
Jun	1990	2	33003	4144	2830	6974
Jul	1990	4	17939	526	1023	1549
Oct	1990	10	8853	671	1006	1677
Jan	1992	2	19958	3515	1965	5480
Feb	1992	2	12819	2574	1758	4332
Mar	1992	1	17564	716	1396	2112
Apr	1992	5	13326	920	891	1811
May	1992	5	14674	686	576	1262
Oct	1992	4	9639	1310	1484	2794
Mar	1993	4	24802	2014	2953	4967
Apr	1993	8	31016	1816	1351	3167
May	1993	15	32379	2438	1329	3767
Jun	1993	6	25293	1171	1263	2434
Aug	1993	3	23069	1223	1021	2244
Sep	1993	1	13909	-	594	-

Ancillary Data

Daily estimates of river discharge for the Mississippi River at Tarbert Landing were obtained from the U.S. Army Corps of Engineers, New Orleans District. In addition, suspended sediment concentration information within the Mississippi River was obtained from the Corps of Engineers and the United States Geological Survey, Baton Rouge Office. These data were used to select the time periods of investigation. They were also used in the regression analyses, after compensating for time-lags between Tarbert Landing and the Mississippi River mouths.

Hourly measurements of wind speed and direction were obtained for the C-man station at Burrwood, situated at the mouth of Southwest Pass. These data were obtained from the National Oceanographic Data Center for the period January 1988 through May 1993. The National Data Buoy Center in Slidell provided data for the period June 1993 through September 1993. The winds were resolved into vector components with oceanographic orientation. East-west components are positive to the east and north-south components are positive to the north. The components were then averaged over the 72, 24, 12, 6 and 3 hours prior to image acquisition. East-west and north-south wind stress was obtained by squaring the wind components.

Tidal information was obtained from the NOAA Tide Tables, U.S. Department of Commerce. The phase of the tide and tidal range were determined for each image. The tidal phase was defined as the time from the last high slack water to the time of image acquisition (after Dinnel et al. 1990).

Statistical Analyses

The SAS^{R} statistical software was used to explore the relationships between environmental variables and the plume parameters. Initially, the most important environmental variables were identified through the use of Pearson product moment correlations and linear regression techniques. Then multiple regression was employed in an attempt to identify relationships which could be used for predictive purposes.

RESULTS

Descriptive Map of the Mississippi River Plume

During year 1 of this study the Mississippi River plume was studied under low, medium, and high river discharge conditions. Low discharge was defined as a flow rate of 0-10,000 $m^3 \cdot s^{-1}$, medium discharge from 10,001-20,000 $m^3 \cdot s^{-1}$, and high discharge from 20,001-35,000 $m^3 \cdot s^{-1}$. In Figure 4, the mean sediment plumes under medium and high discharge conditions are shown (see "C," "B," respectively). The mean plume during medium discharge conditions covered 2165 km^2 of the continental shelf. The mean plume during high discharge conditions covered 3909 km^2. Also shown in Figure 4 is the maximum areal extent of the sediment plume during high discharge conditions. This maximum "composite" plume covered an enormous area of the continental shelf and slope, totalling 13,207 km^2 (Figure 4, "A"). Thus, in the mean, the Mississippi River sediment plume's area was found to be related to large changes in river discharge.

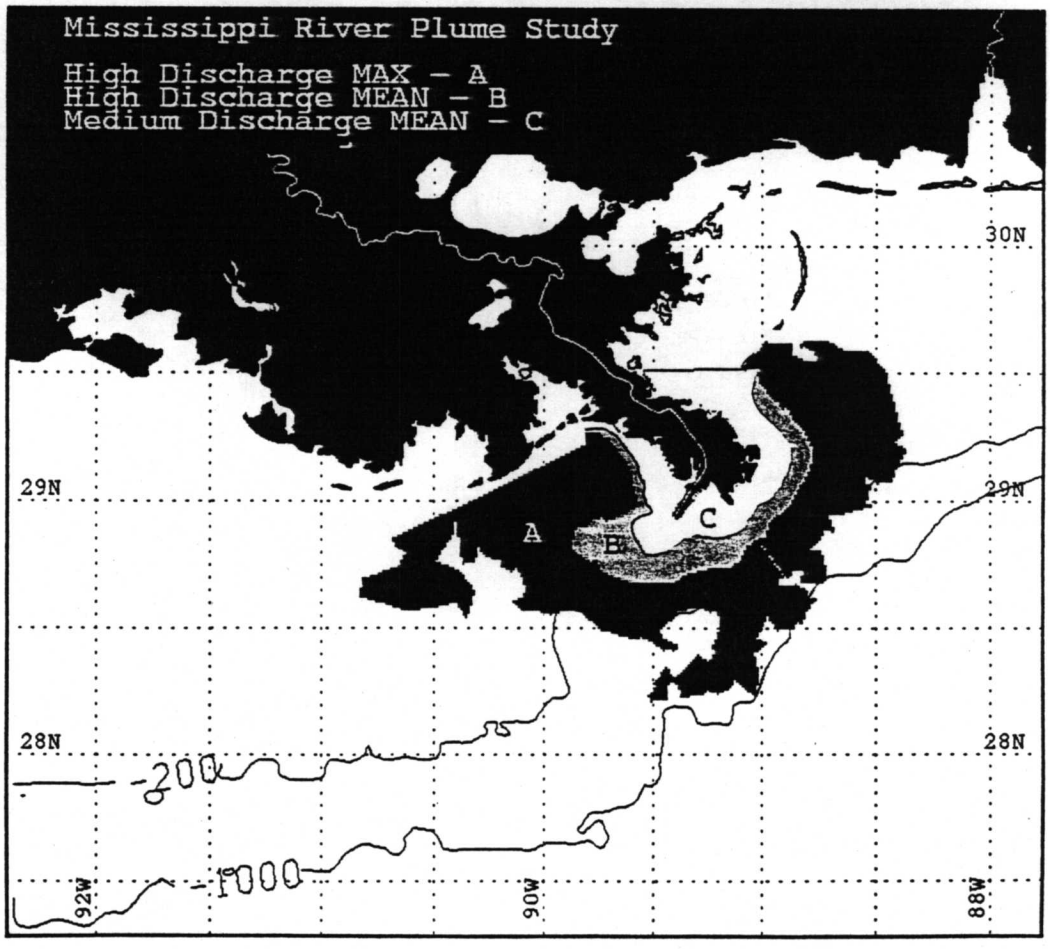

Figure 4. Mississippi River sediment plume composite map summary depicting the mean plume under medium discharge conditions (C), the mean plume under high discharge conditions (B), and the maximum spatial extent of the sediment plume under high discharge conditions (A).

Annual and Interannual Plume Variability

The Mississippi River sediment plume would be expected to vary seasonally as a result of variability in river discharge. Mississippi River discharge (from Tarbert Landing) is shown in Figure 5 for the January 1988 through September 1994 period. Long-term discharge records demonstrate that maximum river discharge occurs from March through May and minimum river discharge occurs from August through October. As an example of the seasonal variability of the sediment plume, resulting mainly from the annual river discharge cycle, the mean plumes for October 1989 and March/April 1989 are illustrated. In October 1989, the mean plume was 2058 km^2 (Figure 6a), whereas, the mean March/April 1989 plume was 4595 km^2 (Figure 6b). In October, the surface sediment concentration did not exceed 10 $mg \cdot l^{-1}$ except very close to the coast. During the March/April period, however, concentrations of 80 $mg \cdot l^{-1}$ were observed where concentrations of 10 $mg \cdot l^{-1}$ were observed in October. River discharge during October 1989 was 9128 $m^3 \cdot s^{-1}$, whereas during March/April 1989 river discharge averaged 28,365 $m^3 \cdot s^{-1}$. Thus, monthly-averaged plume variability is substantially influenced by the annual river discharge cycle.

The interannual variability of the Mississippi River sediment plume was investigated by comparing the average sediment plumes for the springs of 1989, 1990, 1992, and 1993. The year 1991 was excluded as the spring was unusually cloudy over the northern Gulf of Mexico and, therefore, acceptable satellite imagery was very sparse. The average river discharge and plume sizes for each of the four March/April periods are shown in Table 4. The sediment plumes of 1989, 1990, and 1993 were similar in size and morphology. Each of these average spring plumes ranged in concentration from 10 to above 80 $mg \cdot l^{-1}$. The March/April 1992 plume was much smaller and suspended sediment concentrations of the surface plume barely rose above 20 mg l^{-1}. This is not surprising in light of the fact that river discharge in March/April 1992 was almost 1000 $m^3 \cdot s^{-1}$ lower than during the other years. Plume areas for the high discharge springs ranged from an average of 3855 km^2 in 1993 to 4595 km^2 in 1989. The average plume area for the low discharge spring of 1992 was 1836 km^2, less than 50% of the size of the plumes during the other three springs. Suspended sediment contour maps of the four March/April plumes are demonstrated in Figure 7. It is interesting to note that the average plume of March/April 1992 was similar in concentration and morphology to that of October 1989. It is obvious from the suspended sediment contours of the high discharge springs that the strongest gradients in suspended sediment concentration are located along the eastern margin of the plume. The prevailing westward (easterly) wind regime of spring inhibits the eastward dispersal of sediment and results in stronger sediment concentration gradients. In contrast, the sediment concentration gradients on the west side of the plume are much weaker as the plume undergoes buoyant expansion to the west, enhanced by the coriolis force and the "normal" westward flowing coastal current.

Table 4. Interannual variability of spring discharge and plume areas

Year	March/April Discharge ($m^3 \cdot s^{-1}$)	Plume Area West (km^2)	East (km^2)	Total (km^2)
1989	27649	2574	2021	4595
1990	25527	2243	1754	3997
1992	17206	732	1104	1836
1993	27734	1996	1860	3855

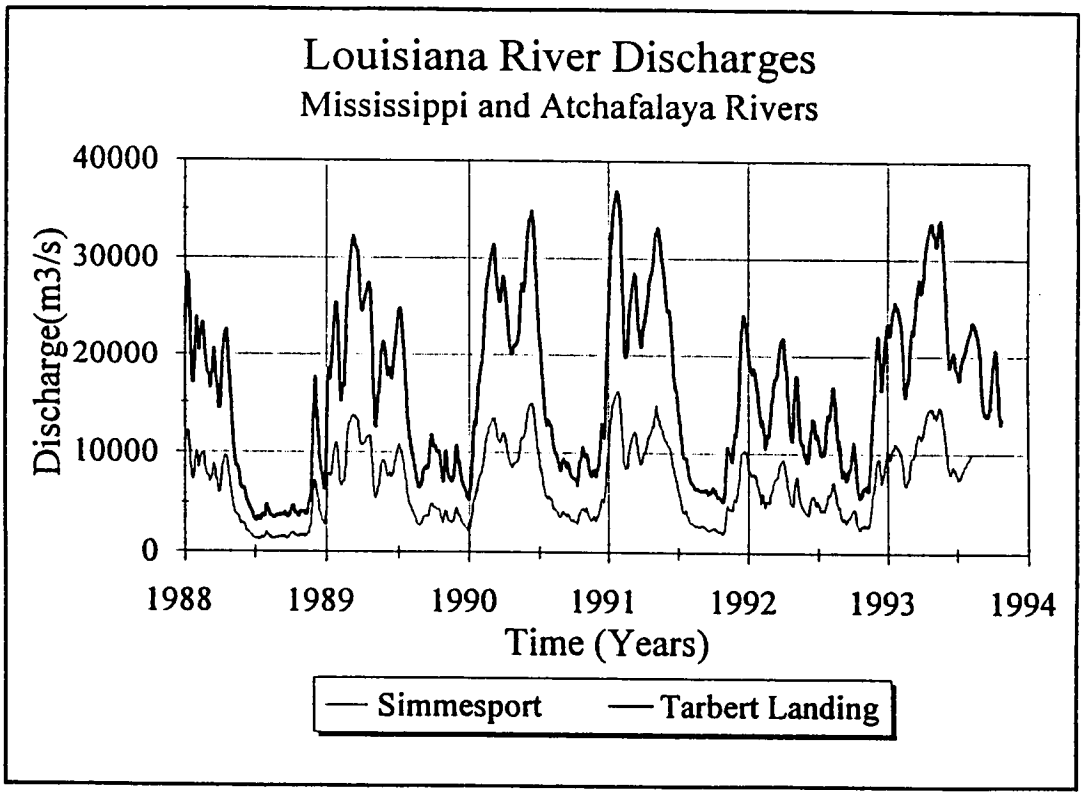

Figure 5. Mississippi River discharge (measured at Tarbert Landing) and Atchafalaya River discharge (measured at Simmesport) from January 1988 through September 1994.

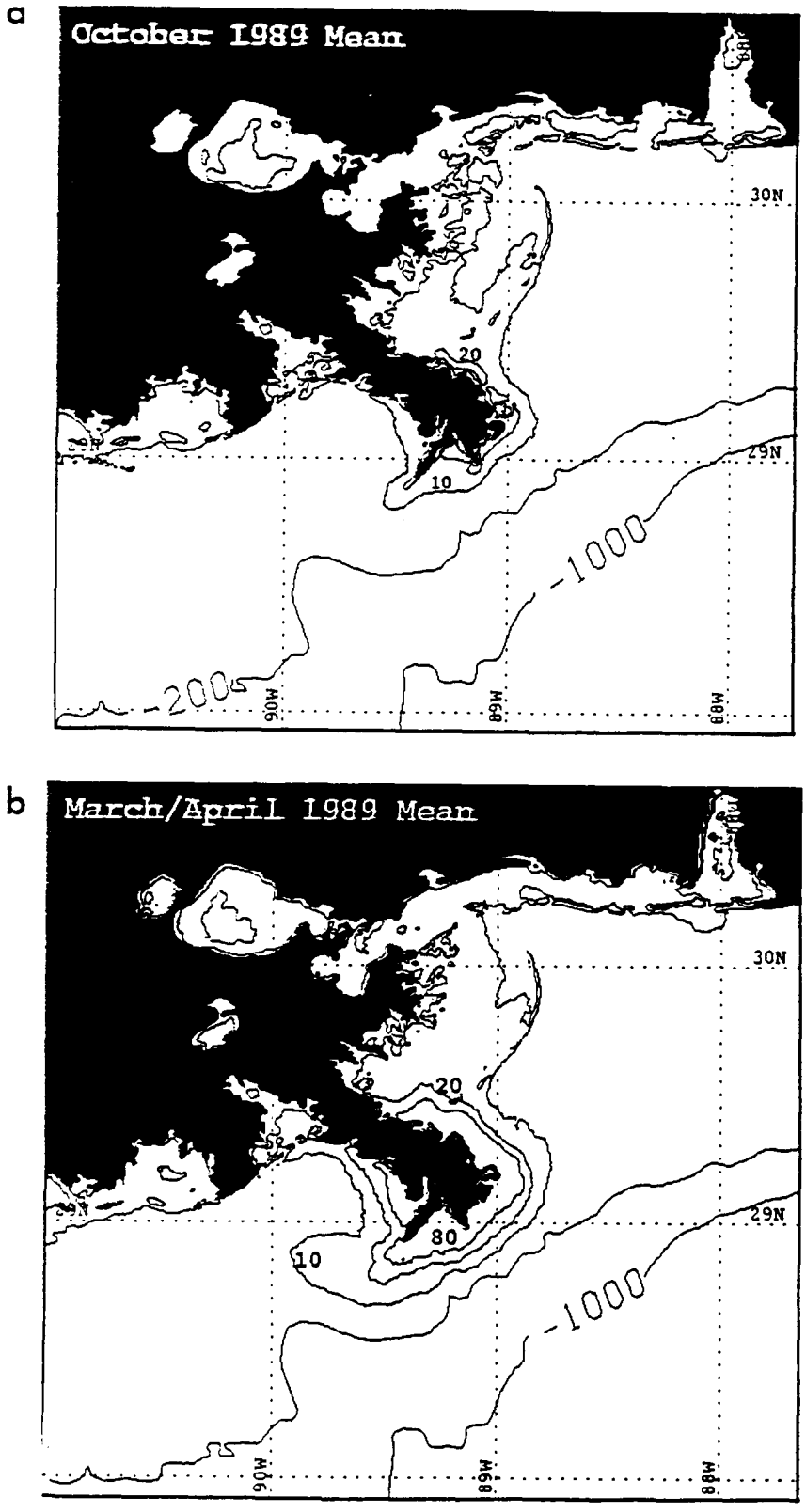

Figure 6. "Average" Mississippi River sediment plumes for a) October 1989 and b) March/April 1989.

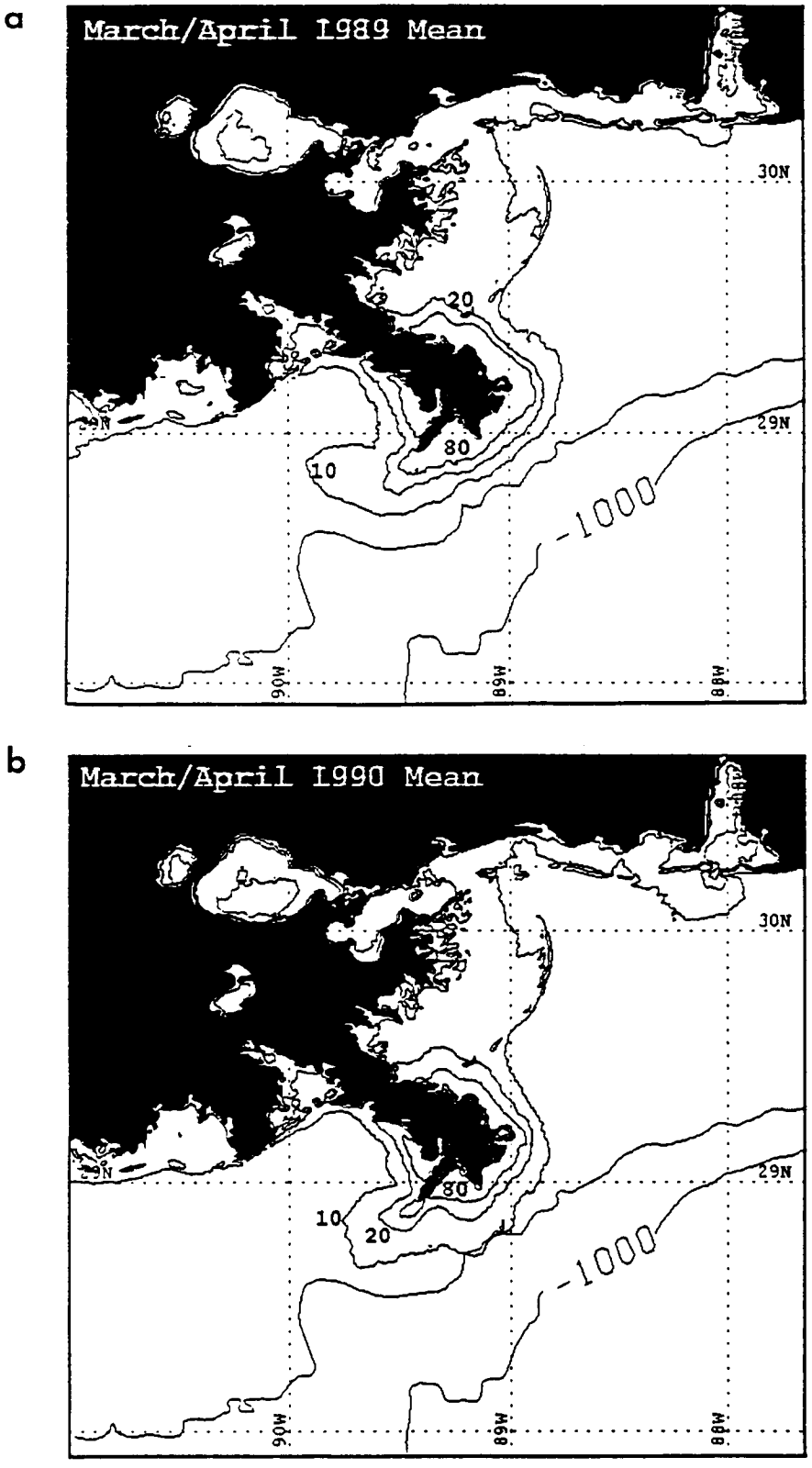

Figure 7. "Average" Mississippi River sediment plumes for a) March/April 1989 and b) March/April 1990.

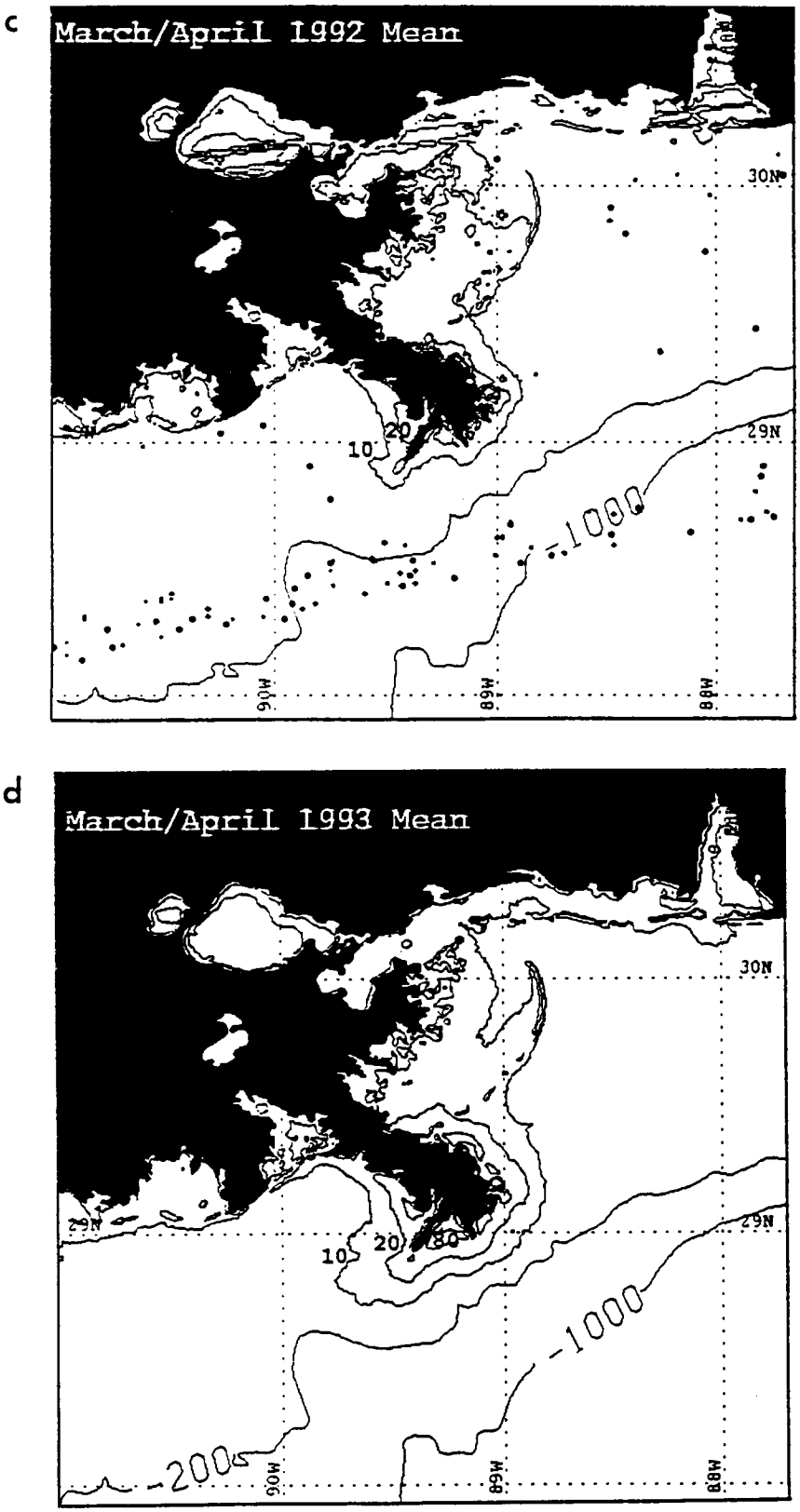

Figure 7. (cont) for c) March/April 1992 and d) March/April 1993.

Forcing Mechanisms for Plume Variability

The plume parameters and environmental variables to be discussed were previously introduced in the methodology section. To assist the reader, the abbreviations for the quantities discussed in the text are listed in Tables 5 and 6.

The relationships between the plume parameters were explored using Pearson product-moment correlations (Table 7). The parameters which showed the highest correlations were AW and DW, with r = 0.85. A similarly high correlation was found for AE and DE. Whereas AE and AW showed a fair positive correlation (r = 0.47), DE and DW were not correlated at all. DS and DW showed a surprisingly high correlation (r = 0.76). The environmental parameters initially included in the statistical analysis were river discharge (RDIS), tidal phase (TP), tidal range (TR), the north-south (NC) and east-west (EC) wind components averaged over 72, 24, 12, 6, and 3 hours prior to image acquisition, and the corresponding north-south and east-west wind stress (square of wind components). Initially, correlation analyses were used to isolate the most important environmental variables. The 12 and 6 hour wind components were found to be better correlated with the plume parameters and, therefore, only their results are shown. In Table 8, the relationships between the most important environmental variables are listed. The highest correlations among the environmental variables were demonstrated by the 12 and 6 hour winds. A significant, albeit weak, relationship was found between the north component of the wind and river discharge. This result suggests a positive relationship between frequency or intensity of northward winds and river discharge. This correlation may reflect the fact that river discharge generally increases (decreases) in spring (autumn) when northward winds become more (less) frequent and/or stronger (weaker). It is interesting to note that a significant negative correlation was observed between river discharge and phase of the tide (TP). This is somewhat surprising as the discharge data were obtained at Tarbert Landing, 480 km from the bird-foot delta.

Table 5. Plume parameters and abbreviations used.

Parameter	Abbreviation
Area East	AE
Distance East	DE
Distance South	DS
Area West	AW
Distance West	DW

Table 6. Environmental variables and abbreviations used.

Variable	Abbreviation
River discharge	RDIS
North wind component	NC
East wind component	EC
Wind speed	WSP
Tidal phase	TP
Tidal range	TR

Table 7. Correlation coefficients (r) between plume parameters. Significance levels are depicted as follows: 99% = '*' 95% = '+' 90% = 'o'. Relationships which are significant at the 90% level or above are shown in bold face.

	AE	DE	DS	AW	DW
AE	—				
DE	**0.82***	—			
DS	**0.43***	**0.29***	—		
AW	**0.47***	0.19	**0.76***	—	
DW	**0.29**	-0.03	**0.48***	**0.85***	—

Table 8. Correlation coefficients (r) between environmental variables. Significance levels are depicted as follows: 99% = '*' 95% = '+' 90% = 'o'. Relationships which are significant at the 90% level or above are shown in bold face.

	RDIS	NC12	EC12	NC6	EC6	TP
RDIS	—					
NC12	**0.27***	—				
EC12	0.07	0.04	—			
NC6	**0.28***	**0.96***	-0.05	—		
EC6	0.10	0.01	**0.96***	0.01	—	
TP	**-0.32***	**-0.16°**	-0.11	-0.11	-0.15	—

The relationships between the plume parameters and environmental variables were first explored using correlation and linear regression techniques. In Table 7 the coefficients of correlation are listed for the most significant relationships obtained using the entire data set. AW was found to be most highly correlated with river discharge (r= 0.55) followed by DS, DW, AE, and DE. All of these correlations were positive and significant at the 95% confidence level. In terms of AW, RDIS was most highly correlated with areal changes and EC winds exhibited the second highest correlations. These results suggest that AW increases (decreases) with increasing (decreasing) river discharge and under the influence of eastward (westward) winds. The relationship between RDIS and AW is shown graphically in Figure 8. The plume measurement, DW, was also primarily affected by RDIS (Figure 9). A very weak negative relationship was found between DW and NC12, indicating that southward (northward) winds may, at times, increase (decrease) the westward extent of the sediment plume.

In terms of AE; RDIS, NC, and EC winds were all significantly correlated with plume area. The sign of these relationships suggests that the eastern plume area increases (decreases) under conditions of increasing (decreasing) discharge, and when northward (southward) and eastward (westward) winds prevail. The scatterplot of RDIS and AE is shown in Figure 10. The eastern extent of the sediment plume (DE) was most strongly correlated with NC12, and less so with RDIS or EC6. The scatterplot and best-fit linear regression for NC12 and DE are illustrated in Figure 11. It is apparent from this plot that when southward winds prevailed (- NC12), plume distances toward the east were generally less than 30 km, whereas under the influence of northward winds (+ NC12), distances ranged from 10-60 km. The explanation which is proposed for this observation is that southward winds, and especially south westward winds, induce a southward flow east of the delta (Walker and Rouse, 1993) which inhibits the eastward flow of river water and sediments. In contrast, the presence of northward winds, particularly those with an eastward component would enhance the eastward extent of plumes east of the delta. The plume measurement, DS, demonstrated significant positive correlations with both RDIS and EC12. The corresponding scatterplot and best-fit linear regression line for DS and EC12 is shown in Figure 12. Under westward wind conditions, sediment plumes were confined

Table 9. Correlations (r) between plume parameters and environmental variables. Significance levels are depicted as follows: 99% = '*' 95% = '+' 90% = 'o'. Relationships which are significant at the 90% level or above are shown in bold face.

All Months

	RDIS	NC12	EC12	NC6	EC6	TP
AW	**0.55***	-0.03	**0.25***	-0.02	**0.26***	-0.13
DW	**0.49***	**-0.17°**	0.01	-0.14	0.03	-0.15
AE	**0.36***	**0.37***	**0.36***	**0.36***	**0.39***	-0.04
DE	**0.27***	**0.52***	**0.25***	**0.49***	**0.27***	0.01
DS	**0.50***	0.11	**0.50***	0.11	**0.48***	-0.17

October - April

	RDIS	NC12	EC12	NC6	EC6	TP	WSP12
AW	**0.59***	-0.11	**0.24+**	-0.10	**0.23+**	-0.15	0.14
DW	**0.54***	-0.17	-0.001	-0.14	0.00	-0.11	0.18
AE	**0.47***	**0.40***	**0.42***	**0.40***	**0.42***	-0.16	0.15
DE	**0.39***	**0.56***	**0.30***	**0.55***	**0.30***	-0.07	-0.01
DS	**0.52***	0.03	**0.48***	0.02	**0.46***	-0.09	0.15

May - September

	RDIS	NC12	EC12	NC6	EC6	TP	WSP12
AW	**0.57***	0.08	0.26	0.07	**0.30°**	-0.02	**-0.40+**
DW	**0.58***	-0.20	0.03	-0.14	0.08	-0.13	**-0.31°**
AE	**0.57***	**0.54***	0.29	**0.44***	**0.39+**	0.28	0.04
DE	0.14	**0.58***	0.18	**0.47***	0.25	**0.32°**	0.02
DS	0.34+	0.12	**0.53***	0.07	**0.52***	-0.19	-0.17

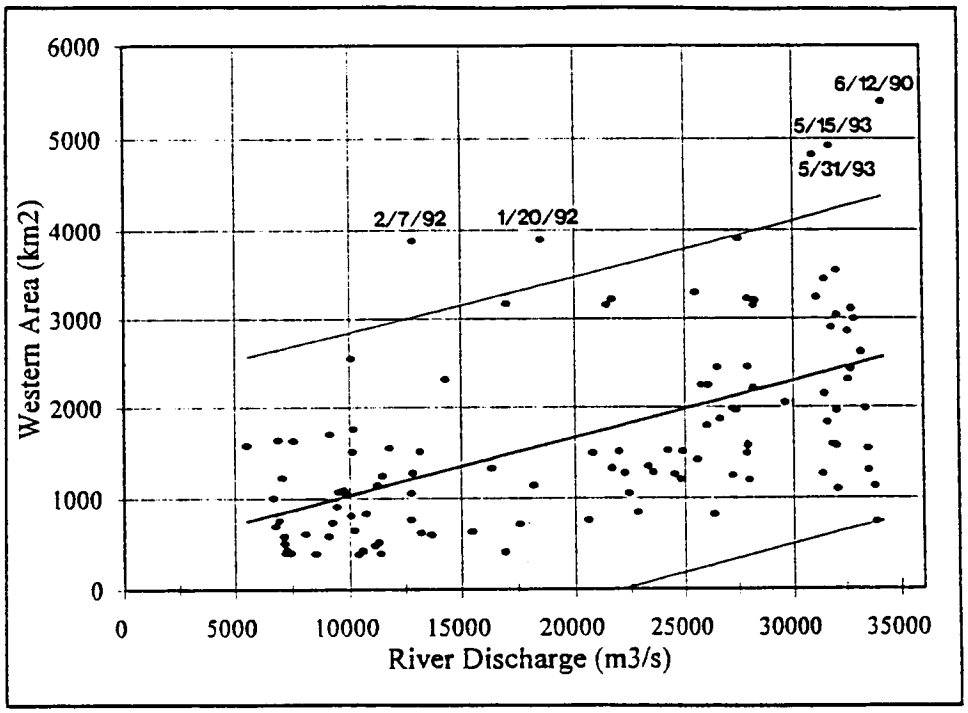

Figure 8. Scatterplot and best-fit regression line for river discharge and area west (AW). The 95% confidence limits are shown with thin solid lines.

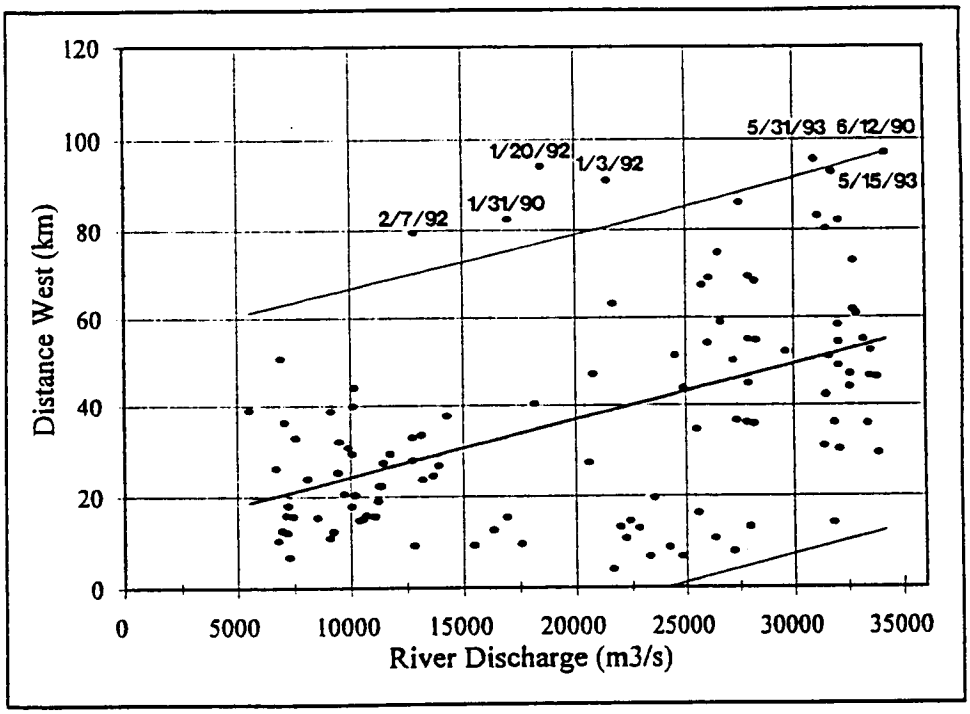

Figure 9. Scatterplot and best-fit regression line for river discharge and distance west (DW). The 95% confidence limits are shown with thin solid lines.

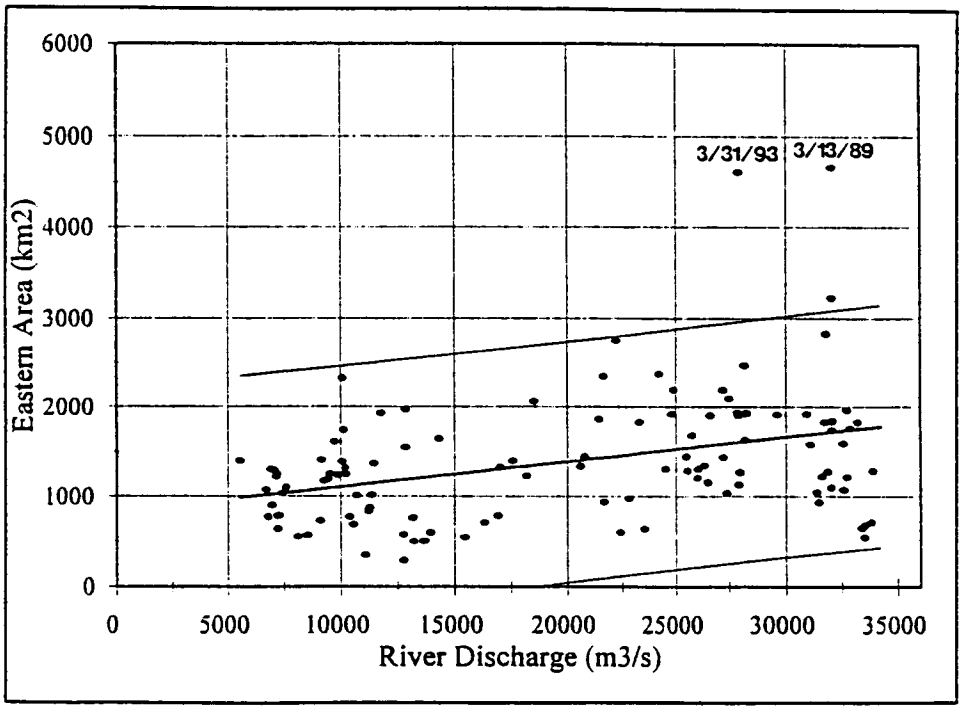

Figure 10. Scatterplot and best-fit regression line for river discharge and area east (AE). The 95% confidence limits are shown with thin solid lines.

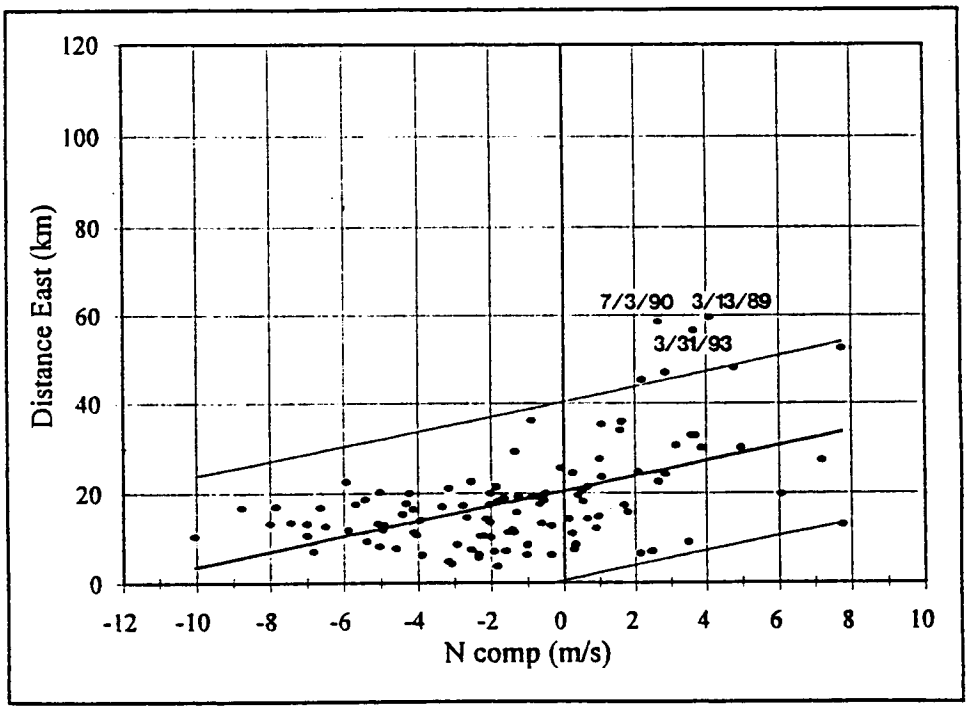

Figure 11. Scatterplot and best-fit regression line for the north-south wind component and distance east (DE). The 95% confidence limits are shown with thin solid lines.

to a distance between 5 and 40 km from Southwest Pass, whereas, under eastward wind conditions plumes ranged from 12 to 85 km from the delta. The outlier points on each of these scatterplots yield considerable information and will be discussed in some detail in the next chapter. It is of interest that no significant correlations were found between any of the plume measurements and tidal phase or range.

In an attempt to explain more of the variation within the plume data set, a detailed investigation of the individual images was made. In particular, the 1993 data set was scrutinized closely. During May 1993, an amazing amount of day-to-day variability in plume areas was observed which appeared to be related to wind speed. For example, a 1826 km^2 plume on 30 May was followed by a 4822 km^2 plume the following day. The only obvious change in the environment was a decrease in wind speed. This was an interesting and curious observation as previous work had suggested a positive relationship between wind speed and plume area, particularly when winds were southward or eastward. At this stage it was hypothesized that stratification of the water column, which increases in spring and is maximized in summer (with increased solar radiation input) may have an important influence on plume dynamics. If this is true, then the relationship between environmental forcing factors and plume morphology may change throughout the year. As no data on strength of stratification is readily available for the satellite image database, the images were divided into a "winter" and "summer" group based on knowledge of seasonal heat balances and their effects on stratification. The satellite images obtained from October through April were considered "winter" images and those from May through September were considered "summer" images. In addition, wind speed (averaged over the 12 hours prior to image acquisition) was included as an environmental variable. The statistical correlations between the plume parameters and the environmental variables were determined with this new split database.

The technique of separating the data base into "summer" and "winter" groups improved most of the resulting correlation coefficients (Table 9). For AW, the positive relationship with river discharge increased, however, the correlations with wind did not improve much. A new significant negative correlation was found between AW and wind speed (WSP12) during the "summer". This suggests that as wind speed increases (decreases), plume area decreases (increases). This, in fact, confirms the qualitative results based on viewing the images. The most probable explanation for this observation is that as wind speed increases, momentum is transferred to the upper layers of the ocean, which breaks down stratification and mixes the sediment through a thicker water column. The net result is that the sediment is more rapidly dispersed downwards in the water column and, thus, less concentrated as a surface plume. Although the relationship between AW and WSP12 during the "winter" was not significant it was of the opposite sign, suggesting that the plume's response to forcing factors may change with season, due to changes in density distribution and stratification between the plume and the ambient shelf waters. Similar results were obtained for DW and WSP12. A negative (non-significant) relationship was observed between DS and WSP12. In contrast, AE and DE were not at all correlated with WSP12. The results indicate that only the western plume area exhibits a significant correlation with wind speed during summer. This may result from the fact that the western side of the plume is more sheltered from the prevailing westward wind and wave regime and, therefore, exhibits more upper layer stratification under low wind conditions.

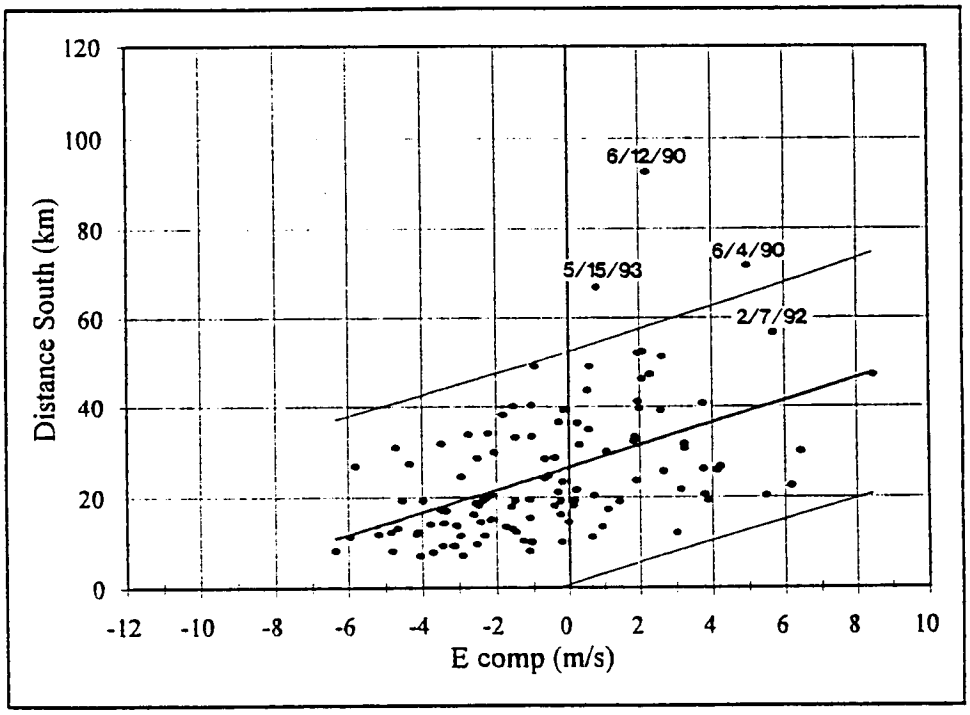

Figure 12. Scatterplot and best-fit regression line for the east-west wind component and distance south (DS). The 95% confidence limits are shown with thin solid lines.

Separation of the images into "summer" and "winter" groups also improved the correlations between AE and most of the environmental variables (Table 9). In particular, during "summer", relatively high correlations were observed between AE and RDIS, NC12, and EC6. This suggests that the eastern plume area increases (decreases) under conditions of high (low) river discharge and under the influence of northward (southward) and eastward (westward) winds. It is interesting to note that DE was only significantly correlated with river discharge during the "winter" months. During both seasons, DE was increased (decreased) primarily by northward (southward) winds and secondarily by eastward (westward) winds. Distance south (DS) was found to be more highly correlated with river discharge in the "winter", however, it was observed to increase (decrease) in the presence of eastward (westward) winds during both seasons.

Multiple Regression Models for Mississippi River Plume Variability

Area West and Distance West

Stepwise multiple regression was used in an attempt to identify models which could be used for predicting plume variability. The best models for each plume measurement are shown in Tables 10 through 14. Variables significant at 90% or above were included in the models shown.

The plume area west of the delta (AW) was found to be most predictable from May through September when 64% of plume variability was explained by RDIS, WSP12, and EC12. RDIS explained about twice the variation of each of the other two variables (Table 10). In simple terms, **during summer months the western plume area increased under conditions of increased river discharge, reduced wind speed, and increased frequency of eastward winds.** The plume area may increase under conditions of reduced wind speeds since buoyant spreading of the plume could occur with minimal vertical mixing of the sediment down through the water column. Thus, the net result would be a plume with a larger surface area. The western area of the plume also increased in size under the influence of eastward winds. Winds from this direction enhance offshore surface flow and, therefore, would assist in re-distribution of the surface sediment plume over a larger area and particular in an offshore direction. The largest plumes west of the delta were observed on 6/12/90 and 5/15/93 (Figure 8) and in both cases the image times were preceded by light to moderate northeastward winds. Suspended sediment contour maps for these two satellite images are shown in Figure 13.

From October through April, 44% of the variance in AW was explained by RDIS, NC12, and EC12 (Table 10). In this case, RDIS explained a dominant portion of the variance. Thus, **during winter the western area of the plume was increased primarily by increased river discharge, and secondarily by increased frequency and/or intensity of southward or eastward winds.** The model for all months was very similar to that of the winter months, however, the variance explained by the environmental variables was reduced to 39%. Although the effect of the wind in these latter two cases was not great, the relationships can be explained physically. Winds blowing towards the southeast, typical of winter frontal passage episodes, enhance offshore transport of surface waters with the ultimate effect of spreading the sediment plume seaward. Southwestward winds would enhance the prevailing westward flow of water along the coast, thus extending the plume towards the west. The multiple regression results of DW support this contention. The model results for DW were very similar to those for AW except that eastward winds did not help explain any of the variance for DW (Table 11). Thus, although eastward winds enhanced plume area west of the delta they inhibited the westward extent of the sediment plume. For the winter months and for all months, most of the variance in DW was explained by river discharge and a smaller portion by NC12. **The western extent of the plume was maximized when river discharge was high and when southward winds increased in strength and/or frequency. During the summer months, under conditions of greater stratification of the water column, wind speed became important. As was found for the western area in summer, the length of the plume westward was enhanced somewhat by a reduction in wind speed.** The apparent relationship with wind speed may only be relevant to the methodology used here. The satellite sensor views only the upper meters of the water column in the visible band and, thus, the sediment is not detectable by the satellite sensor once

Table 10. Best multiple regression models for area west (AW)

May - September (n = 34)

Variable	Partial R^2	Model R^2	Prob > F
+ RD1S	0.32	0.32	0.0004
- WSP12	0.17	0.49	0.0027
+ EC12	0.15	0.64	0.0010

Eq: Y = 0.11 (RD1S) - 265 (WSP12) + 166 (EC12) + 157

October - April (n = 76)

Variable	Partial R^2	Model R^2	Prob > F
+ RD1S	0.35	0.35	0.0001
- NC12	0.07	0.42	0.0052
+ EC12	0.03	0.45	0.0715

Eq: Y = 0.07 (RD1S) - 61 (NC12) + 53 (EC12) + 367

All Months (n = 111)

Variable	Partial R^2	Model R^2	Prob > F
+ RD1S	0.31	0.31	0.0001
+ EC12	0.05	0.36	0.0067
- NC12	0.03	0.39	0.0198

Eq: Y = 0.07 (RD1S) + 73 (EC12) - 56 (NC12) + 283

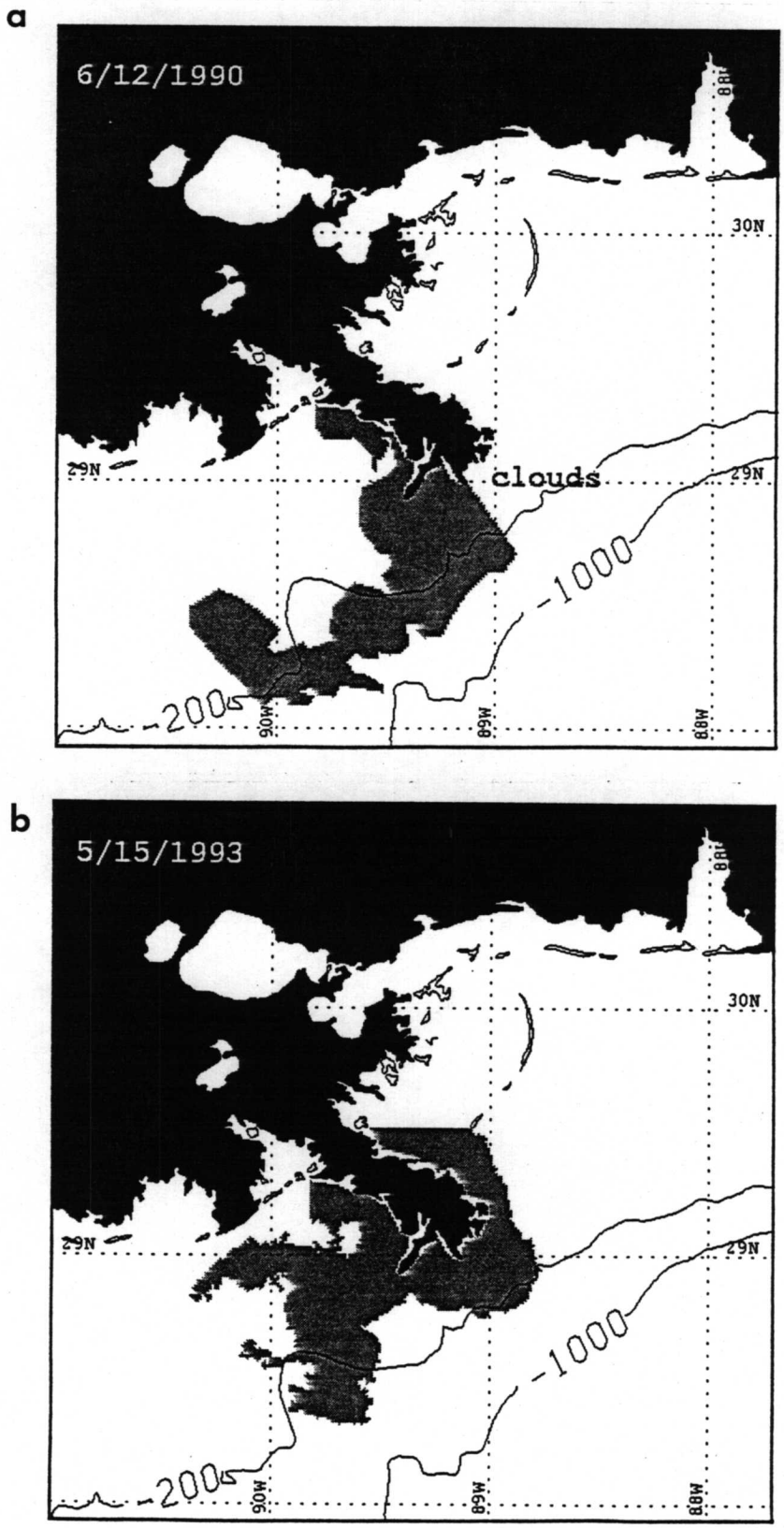

Figure 13. Mississippi River sediment plume as revealed in NOAA satellite imagery from a) 06/12/90 and b) 05/15/93.

Table 11 Best multiple regression models for distance west (DW)

May - September (n = 35)

Variable	Partial R^2	Model R^2	Prob > F
+ RD1S	0.33	0.33	0.0003
- WSP12	0.11	0.44	0.0138
- NC12	0.10	0.54	0.0154

Eq: Y = 0.002 (RD1S) - 4.45 (WSP12) - 3.36 (NC12) - 3.2

October - April (n = 76)

Variable	Partial R^2	Model R^2	Prob > F
+ RD1S	0.30	0.30	0.0001
- NC12	0.09	0.39	0.0011

Eq: Y = 0.0015 (RD1S) - 1.84 (NC12) + 7.3

All Months (n = 112)

Variable	Partial R^2	Model R^2	Prob > F
+ RD1S	0.24	0.24	0.0001
- NC12	0.10	0.34	0.0001

Eq: Y = 0.0015 (RD1S) - 2.23 (NC12) + 4.2

it drops out of the surface waters. In reality, the sediment plume may exist sub-surface. Previous work has shown that the maximum sediment concentration may lie beneath the surface at the top of the pycnocline. (Wright 1970).

The satellite imagery of 01/20/92 and 02/07/92 aptly demonstrate plume morphology after prolonged episodes of southwestward and southeastward winds (Figure 14) associated with winter cold front passages. Although both satellite images occurred during a period of medium discharge (10,000-20,000 $m^3 s^{-1}$), the sediment plumes were some of the largest observed west of the delta, approaching 4000 km^2. Plume morphology was distinctly different in the two images, as on 2/7/92 the plume extended southwestward from the "bird-foot" delta region, whereas, on 1/20/92 the plume recurved towards the coast, essentially colliding with the coast between Barataria and Terrebonne Bays. The western extent of each plume was also impressive. That of 1/20/92, followed a strong episode of southwestward winds, and was thus particularly long, extending 95 km from the delta. It is interesting to note that both of these images were outlier points on the scatterplots of AW and RDIS (Figure 8) as well as DW and RDIS (Figure 9).

Distance South

The best model for DS was obtained during May through September, when 53% of the variance was explained by EC12, RDIS, and WSP12 (Table 12). In this case, the most variance (29%) was explained by the wind component EC12 whereas the variance explained by RDIS dropped to 15%. As was observed for the western plume parameters in summer, plume length was greatest under low wind speed conditions. **Thus during summer plume length towards the south increased in association with eastward winds, increasing discharge, and reduced wind speeds.**

Similar results were obtained for the October-April group and the annual group, however, no relationship with wind speed was observed. In both cases, RDIS and EC12 explained similar amounts of the variance. **Thus, the southern extent of the sediment plume was maximized during winter when the intensity and/or frequency of eastward winds increased and when river discharge increased.** The effect of eastward winds on offshore movement of the surface sediment plume is not surprising in light of previous work on circulation in the northwestern Gulf of Mexico. Cochrane and Kelly (1986) demonstrated that shelf currents respond most rapidly to along shore wind stress. Thus, the offshore transport of surface waters would be enhanced under eastward wind conditions, primarily due to Ekman dynamics. In the presence of eastward and northeastward winds, the Southwest Pass plume was forced southwards. The satellite images of 6/4/90 and 5/13/93 provide good examples of the plume's surface morphology under conditions of strong eastward winds (Figure 15).

Table 12. Best multiple regression models for distance south (DS)

May - September (n = 35)

Variable	Partial R^2	Model R^2	Prob > F
+ EC12	0.29	0.29	0.0007
+ RD1S	0.15	0.44	0.0050
- WSP12	0.08	0.53	0.0234

Eq: Y = 3.63 (EC12) + 0.001 (RD1S) - 2.34 (WSP12) + 169

October - April (n = 76)

Variable	Partial R^2	Model R^2	Prob > F
+ RD1S	0.27	0.27	0.0001
+ EC12	0.19	0.46	0.0001

Eq: Y = 0.0006 (RD1S) + 1.78 (EC12) + 12.5

All Months (n = 112)

Variable	Partial R^2	Model R^2	Prob > F
+ RD1S	0.25	0.25	0.0001
+ EC12	0.21	0.46	0.0001

Eq: Y = 0.0007 (RD1S) + 2.3 (EC12) + 11.52

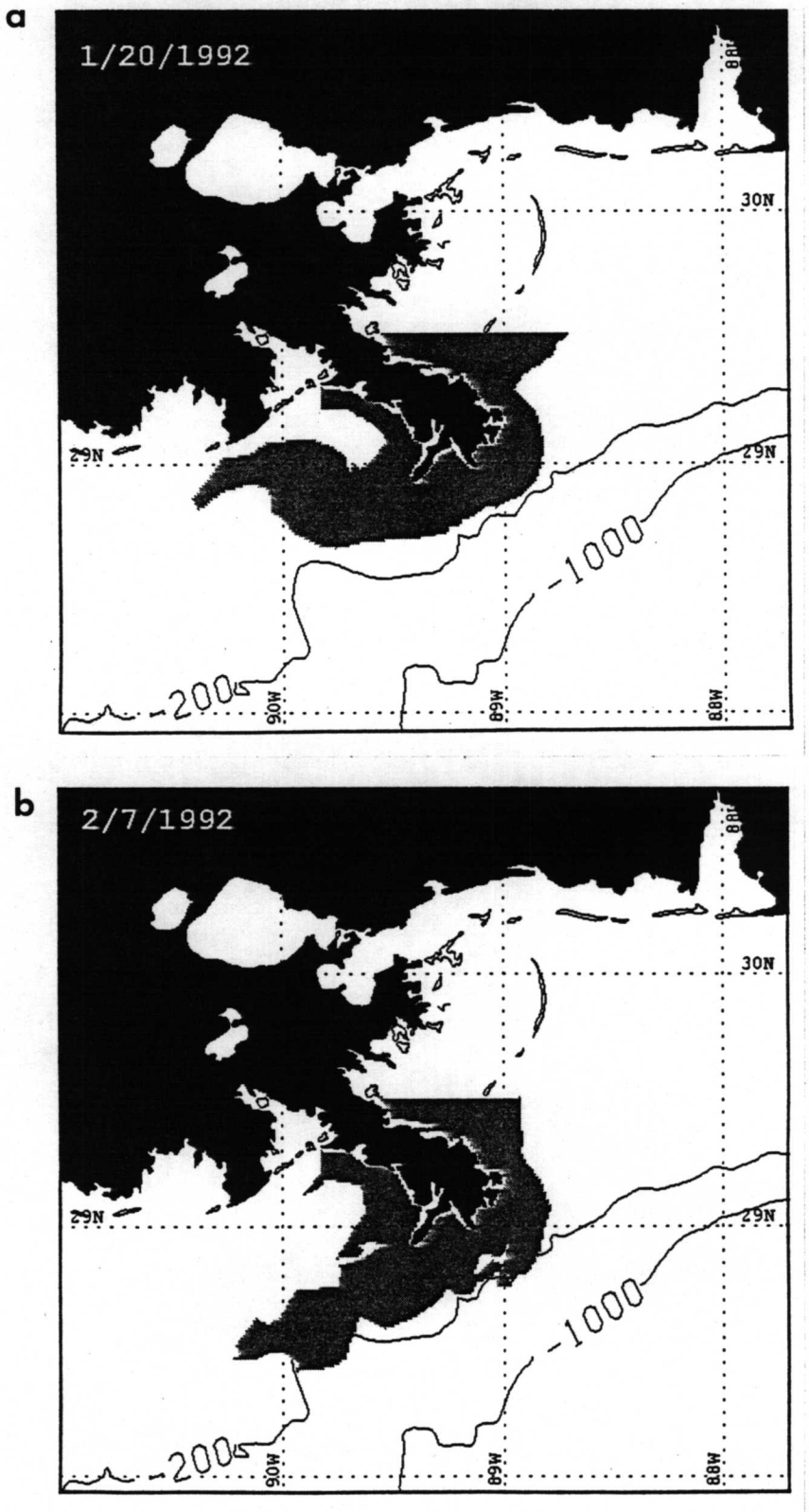

Figure 14. Mississippi River sediment plume as revealed in NOAA satellite imagery from a) 01/20/92 and b) 02/07/92.

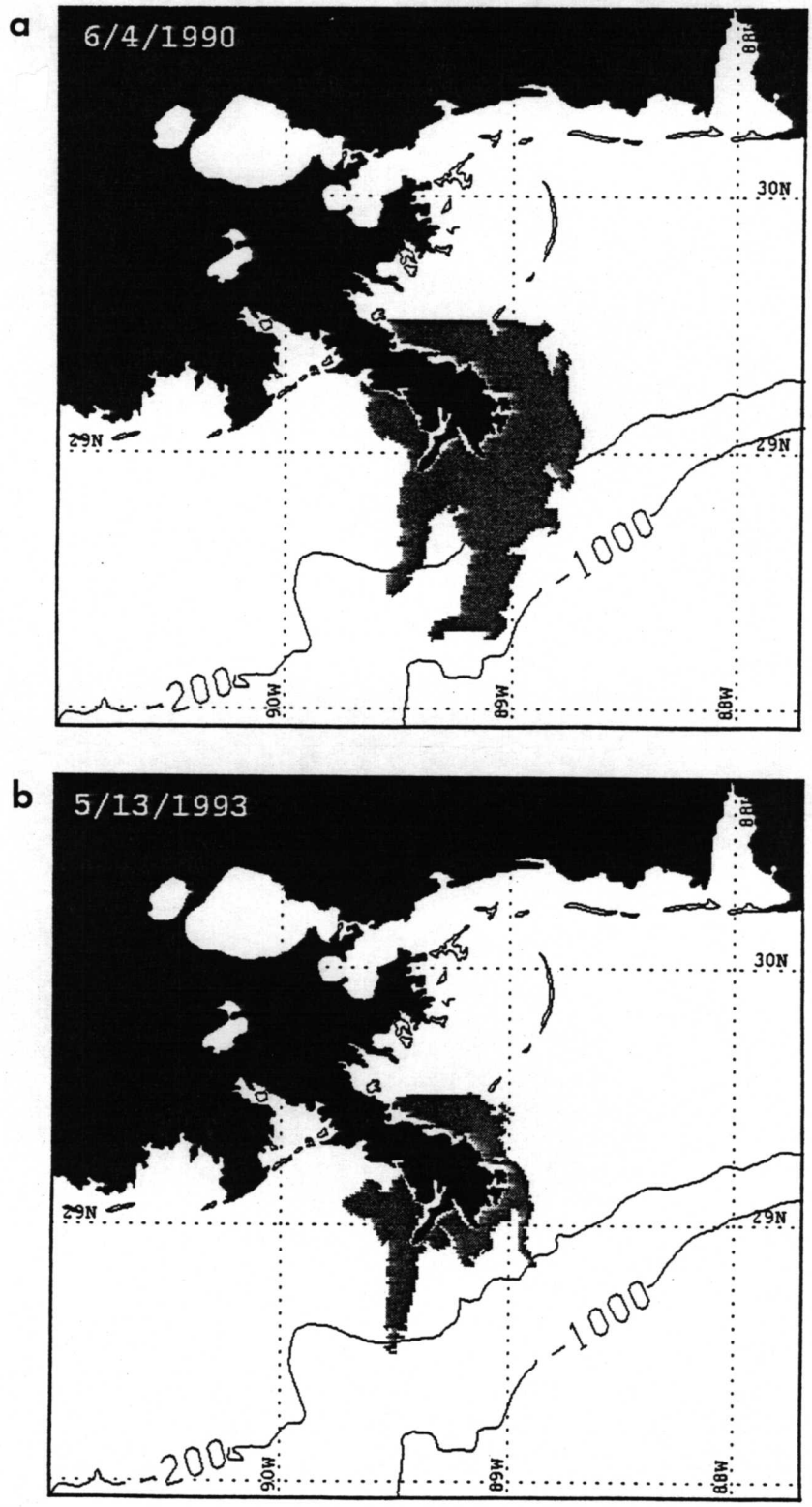

Figure 15. Mississippi River sediment plume as revealed in NOAA satellite imagery from a) 06/04/90 and b) 05/13/93.

Area East and Distance East

The model for the eastern area of the plume (AE) during the summer period was particularly impressive explaining 70% of the variance. The environmental variables of importance were RDIS which explained 34% of the variance, NC12 which explained 22% of the variance, and EC12, which explained 14% of the variance (Table 13). **Thus, the plume area east of the delta was increased during summer when river discharge increased and when northward and/or eastward winds prevailed.** The amount of variance explained by the environmental variables decreased for the winter and annual groups, however, the same environmental variables were responsible for plume variability. During the October through April period, 49% of the variance was explained by RDIS, EC12, NC12, and WSP12. A small portion of the variance was explained by wind speed and, in this case, higher wind speeds corresponded with larger plumes. When considering all of the months together, the model explained 34% of the variability in plume area.

When considering the eastern extent of the plume, river discharge explained comparatively little of the variance. In contrast, NC12 explained most of the variance in plume variability and EC12 played a secondary role (Table 14). The best model in this case was that of October through April when 48% of the variance was attributable to the environmental variables. **Thus, the eastward extent of the sediment plume was increased mainly by the prevalence of northward winds, secondarily by eastward winds, and lastly by increased river discharge.**

The satellite images of 3/13/89 and 3/31/93 aptly demonstrate how the tandem occurrence of high river discharge and northeastward winds can maximize plume area east of the delta (Figure 16). Plume areas for these two cases were 4668 km^2 and 4613 km^2. Another good example of the effects of eastward winds occurred during August 1993. The next section has been dedicated to this event.

Table 13. Best multiple regression model for area east (AE)

May - September (n = 32)

Variable	Partial R^2	Model R^2	Prob > F
+ RD1S	0.34	0.34	0.0003
+ NC12	0.22	0.56	0.0006
+ EC12	0.14	0.70	0.0010

Eq: Y = 0.46 (RD1S) + 109.2 (NC12) + 72.7 (EC12) + 25.1

October - April (n = 76)

Variable	Partial R^2	Model R^2	Prob > F
+ RD1S	0.22	0.22	0.0001
+ EC12	0.14	0.35	0.0002
+ NC12	0.12	0.47	0.0001
+ WSP12	0.02	0.49	0.0755

Eq: Y = 0.024 (RD1S) + 99.3 (EC12) + 79.4 (NC12) + 52.3 (WSP12) + 971

All Months (n = 109)

Variable	Partial R^2	Model R^2	Prob > F
+ NC12	0.13	0.13	0.0001
+ EC12	0.14	0.28	0.0001
+ RD1S	0.06	0.34	0.0022

Eq: Y = 62.1 (NC12) + 86.3 (EC12) + 0.02 (RD1S) + 1125.3

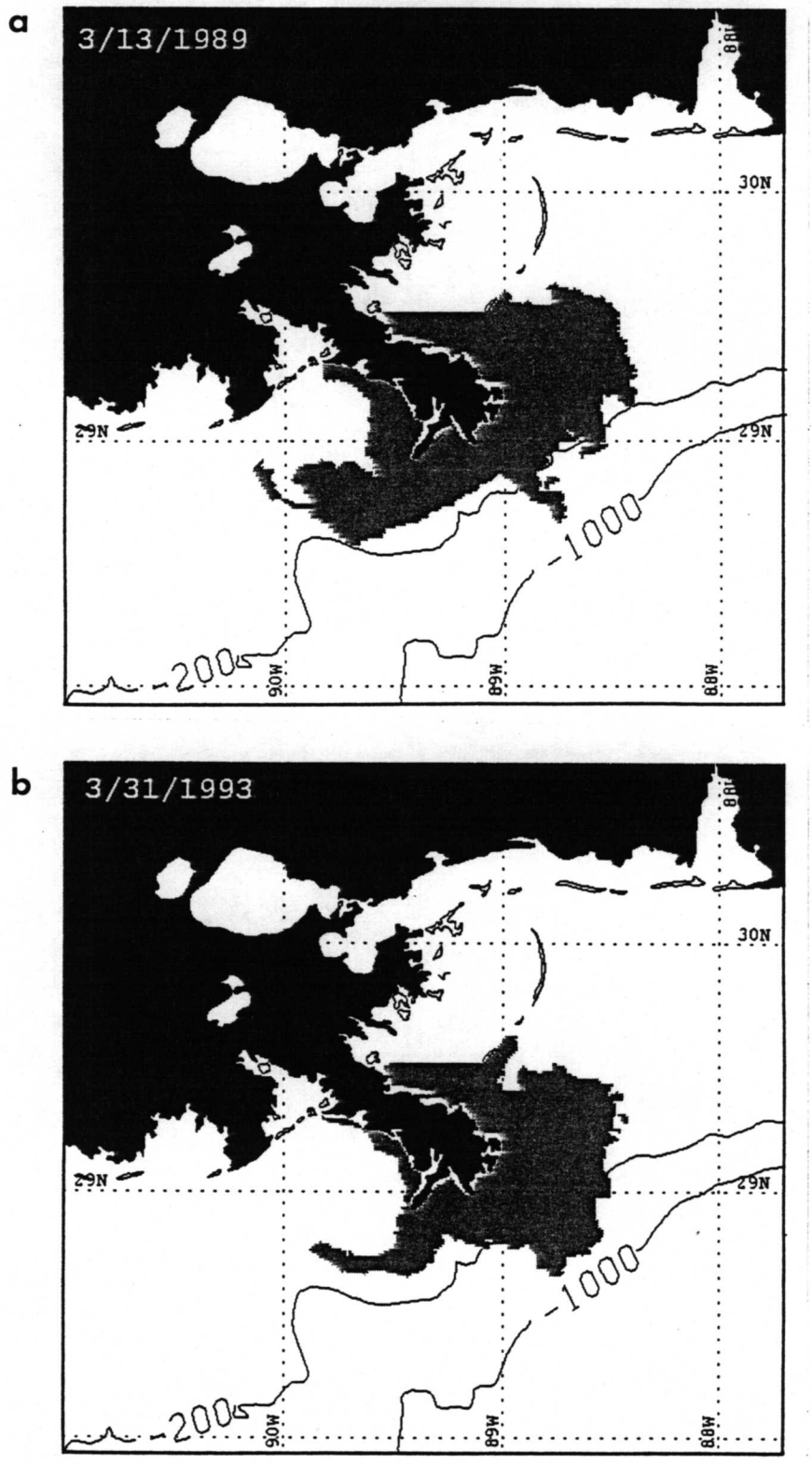

Figure 16. Mississippi River sediment plume as revealed in satellite imagery from a) 03/13/89 and b) 03/31/93.

Table 14. Best multiple regression model for distance east (DE)

May - September (n = 34)

Variable	Partial R^2	Model R^2	Prob > F
+ NC12	0.33	0.33	0.0003

Eq: Y = 2.86 (NC12) + 17.7

October - April (n = 76)

Variable	Partial R^2	Model R^2	Prob > F
+ NC12	0.32	0.32	0.0001
+ EC12	0.11	0.43	0.0003
+ RD1S	0.05	0.48	0.0079

Eq: Y = 1.53 (NC12) + 1.18 (EC12) + 0.0003 (RD1S) + 17.38

All Months (n = 111)

Variable	Partial R^2	Model R^2	Prob > F
+ NC12	0.27	0.27	0.0001
+ EC12	0.08	0.35	0.0005
+ RD1S	0.02	0.37	0.0485

Eq: Y = 1.69 (NC12) + 1.12 (EC12) + 0.0002 (RD1S) + 13.5

A Case Study of River Circulation Associated with the Great Flood of Summer 1993

During the summer of 1993, the Mississippi River basin in the midwestern U.S.A. experienced anomalously high rainfall. Record flooding resulted from an abnormally persistent atmospheric weather pattern consisting of a quasi-stationary jet stream positioned over the central U.S., where moist unstable air flowing north from the Gulf of Mexico converged with unseasonably cool, dry air moving south from Canada. In concert with the persistent weather pattern over the U.S., highly anomalous circulation patterns were observed over much of the Northern Hemisphere (Richards, 1994). The rainfall anomalies over the central U.S. produced abnormally high river discharges along the Louisiana coastline from the Mississippi and Atchafalaya Rivers during July and August, usually months of low river discharge.

The monthly mean discharges of 1993 are compared with long-term climatological values (1930-1992) of minimum, mean, and maximum discharges in Figure 17. This data analysis reveals that monthly mean discharges were above normal during the first 9 months of 1993. Monthly mean discharges of April and May 1993 were approximately 50% higher than their respective long-term monthly mean values. August and September 1993 discharges exceeded those of the previous 63 years! Discharge in August 1993 exceeded that of an average month during the annual spring flood.

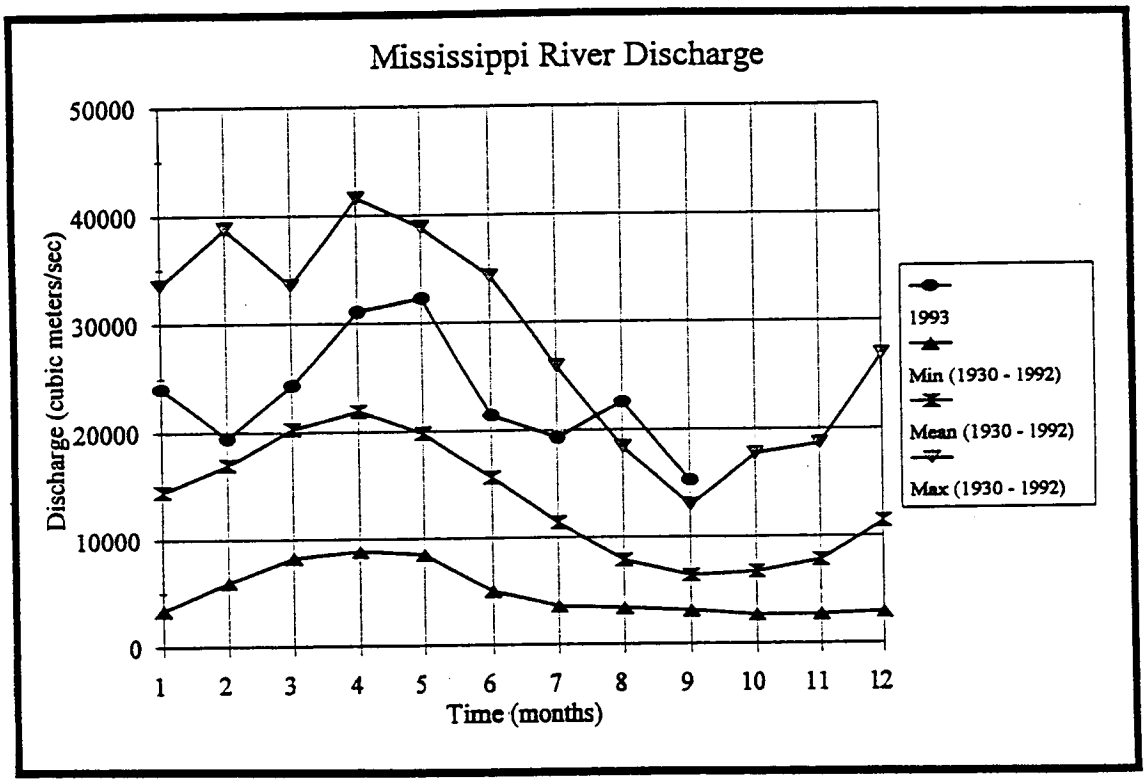

Figure 17. Monthly averaged Mississippi River discharge during January-September 1993 in comparison with long-term climatological values (63 years) of minimum, mean, and maximum discharge.

During the 1993 summer, not only was river discharge anomalously high but the direction of flow of river water in the northern Gulf of Mexico was also unusual. During the 1993 summer, persistent eastward flow of river water was observed in cloud-free satellite imagery. On August 10, an enormous plume of turbid river water was detected extending eastward from the Mississippi River delta region. River water discharged on the western side of the delta flowed eastward around the south side of the delta, joining river water discharged from passes on the south and east sides of the delta. The sediment plume (defined by sediment concentrations > 6 $mg \cdot l^{-1}$) was observed to cover 7000 km^2, extending 270 km eastward onto the Mississippi, Alabama, and Florida continental shelves to 87°30' W. The Research Vessel GYRE traversed portions of the plume from August 6 to 9 en route to Panama City, Florida from Galveston, Texas. Surface salinity measurements obtained underway revealed several areas of low salinity surface water east of the delta (Doug Biggs, personal communication, Walker et al., 1994). A minimum salinity value of 15 (psu) was encountered at the eastern margin of the Mississippi sediment plume as observed on 10 August 1993 (Figure 18, "A"). Although cloud-cover east of "A" prohibited tracking the sediment plume, the salinity measurements suggested the presence of Mississippi River water as far east as 86°40' W. The shipboard measurements also revealed an extensive area of low salinity water (18-25 psu) west of the Mississippi River delta (Figure 18, "B"). This water was probably discharged onto the shelf by the Atchafalaya River and driven eastward by the wind.

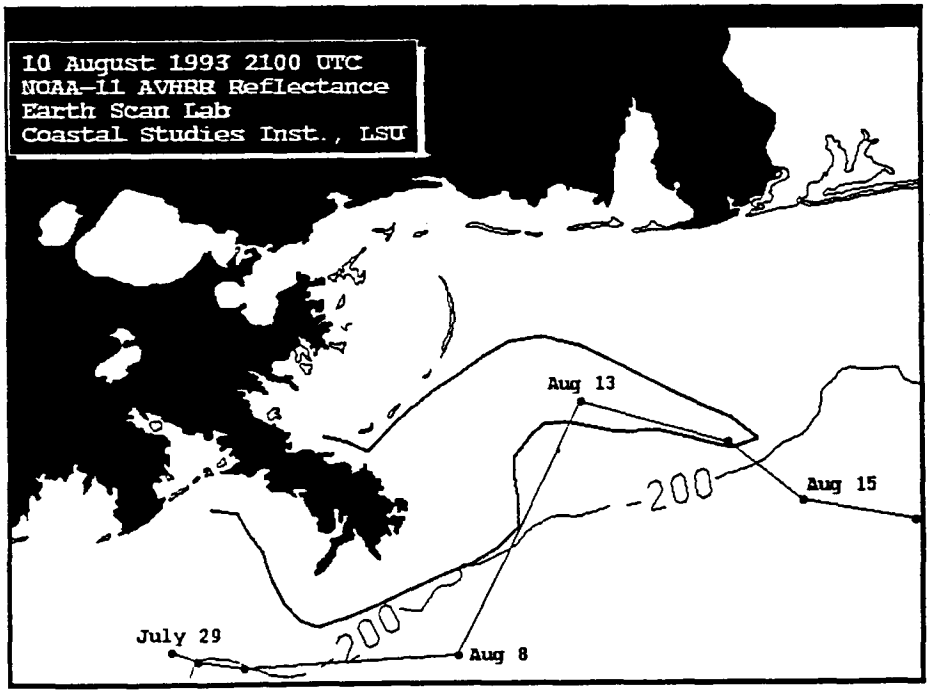

Figure 18. Mississippi River sediment plume on 08/10/93 and track of LATEX-A drifting buoy #6935. Lighter shades of grey indicate higher surface suspended sediment concentrations. The plume waters exhibiting the lowest salinities were encountered at A and B.

Wind measurements at Burrwood, Southwest Pass, LA suggest that the eastward flow of river water was at least partially wind-driven. From mid-July through the third week in August, winds along the Louisiana coast were predominantly eastward and northeastward (Figure 19), which would have driven the buoyant plume towards the east. Thus, the persistence of eastward winds during July and August 1993 effectively reversed the westward flow of Mississippi River water and forced the buoyant plume to the east. This case study further supports the statistical results, presented in the previous section, which demonstrated the importance of the prevailing winds to the circulation of river water in the northern Gulf of Mexico.

Another important factor influencing circulation of Mississippi River water during the 1993 summer was anticyclonic flow along the northern margin of the Loop Current. The Loop Current, a branch of the Yucatan-Florida Current system, had recently intruded northwards in close proximity to the Mississippi delta, introducing eastward flow over the continental slope and outer continental shelf possibly enhancing the rapid eastward movement of river water. Hydrographic measurements, obtained from the R/V Pelican during a Gulf of Mexico Cetacean Survey (GulfCet) south and east of the delta in late August, confirmed the presence of anticyclonic transport along the northern margin of the Loop Current, from 90^0 to 88^0 30' W between the 100 and 2000 m isobaths (Giulietta Fargion, personal communication; Walker et al., 1994). Eastward transports of 4-6 x 10^6 $m^3 \cdot s^{-1}$ were estimated from geopotential heights calculated from cruise measurements along lines southeast and southwest of the Mississippi River. Salinity measurements obtained along the 100 m isobath revealed the river discharge plume to be a thin lens (< 5 m thick) of fresher water (< 25 psu) overlying relatively saline water (36 psu) at 30 m depth. The fraction of freshwater within the top 3 m (reference level of 36.56 psu) was computed at each cruise station (methodology following Dinnel and Wiseman, 1986) revealing a maximum value of 56% east of the delta. Moving eastward, the freshwater fraction remained above 20% to 87 30' W and seaward to the 2000 m contour. The values east of the delta were approximately double those obtained in August 1992 in the same region.

Drifting buoys were deployed west of the delta in late July as part of the Minerals Management Service (MMS) sponsored Texas-Louisiana Shelf Circulation and Transport Processes Study (LATEX-A). The drift tracks confirmed the prevalence of eastward surface flow along the continental shelf around the Mississippi River delta from late July through late August. Two of the drifters moved around the south side of the delta and were caught up in the turbid, low salinity plume extending eastward from the bird-foot delta (as observed on August 10). Both drifters were observed to jog northeastward east of the delta, either due to a wind-induced current or a small anticyclonic eddy impinging on the continental shelf southeast of the delta. From August 13 to 19, drifter #6935 moved eastward between the 200 m and 1000 m isobaths at a velocity of 50-60 cm/s, then continued southward along the west Florida shelf, reaching the Florida Straits by 20 September (Walker et al. 1994). Drifter #6937 was detained west of Tampa along the shelf break, apparently caught up in small eddies, and never reached the Florida Key region. A third LATEX drifter traveled over the continental slope, closer to the axis of the Loop Current, and reached the Florida Keys in early September.

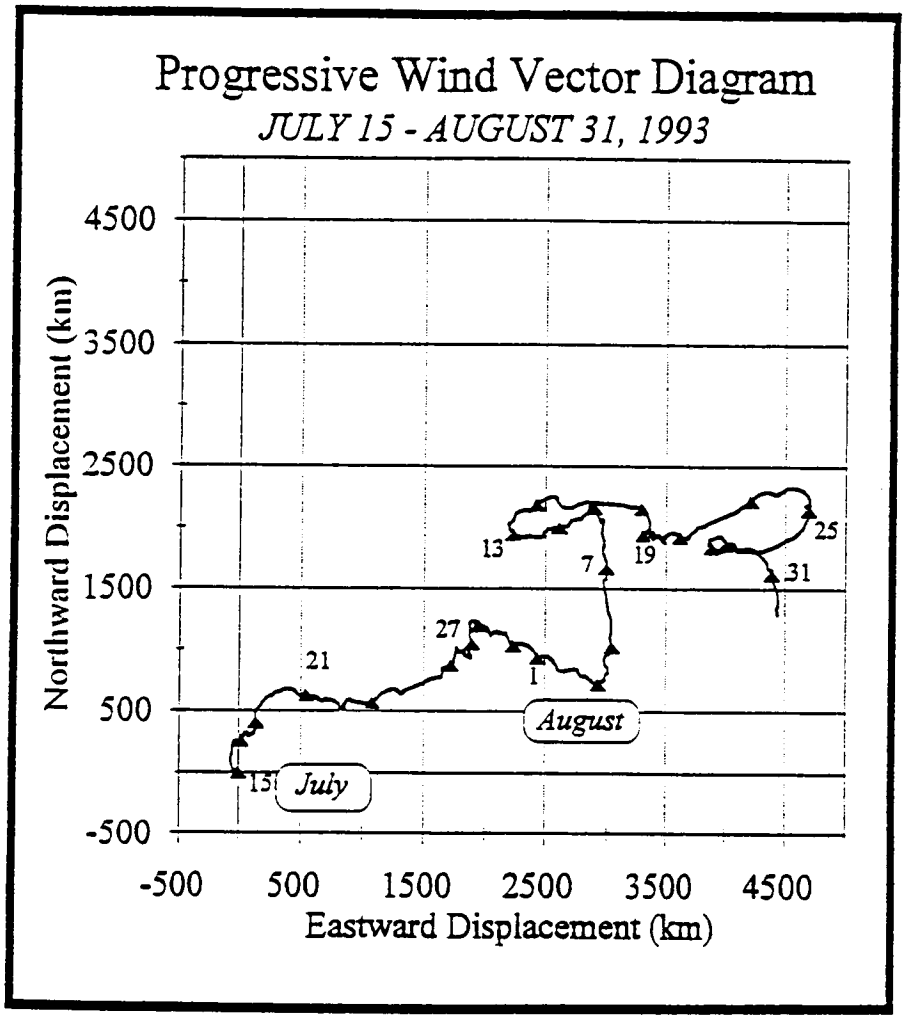

Figure 19. Wind displacement at Burrwood, Southwest Pass from 07/15/93 through 08/31/93.

The drifter tracks help explain observations of unusually low salinity water in the Florida Key region and on the inshore edge of the Florida Current from September 9 to 13 (Gilbert et al., 1994; Lee et al., 1994). Low salinity water was also encountered along the U.S. east coast off North Carolina on September 22 (Tester and Atkinson, 1994). The available data suggest that currents favorable for eastward and southward flow of river water in the northeastern Gulf of Mexico were present for at least six weeks from mid-July through late August. The satellite imagery, hydrographic measurements, and drifter data support the contention that the low salinity water encountered in the northeastern Gulf of Mexico, south Florida region, and along the east coast of the U.S. during the 1993 summer was of Mississippi River origin. Low salinity water has previously been reported along the U.S. east coast (Atkinson and Wallace, 1975) and hypothesized to be of Mississippi River origin. Its movement from the northern Gulf of Mexico through the Florida Straits and up the U.S. east coast was also linked to a northward incursion of the Loop Current. This previous event occurred during 1973, another year of high river discharge. Northward intrusions of the Loop Current, as occurred during the 1993 summer, can occur several times each year and, thus, are not, in and of themselves, unusual occurrences. What was anomalous in 1993 was the simultaneous occurrence of high river discharge onto the Louisiana continental shelf, the abnormal persistence of westerly winds along the Louisiana

coastline, and the prevalence of anticyclonic Loop Current transport in close proximity to the Mississippi River delta. These three factors ensured that a detectable amount of river water reached the Florida Keys and the east coast of the U.S., entrained on the inshore margin of the Loop and Florida Currents. This circulation process probably occurs on a smaller scale much more often than has been previously detected.

Some of the consequences of the Mississippi River flooding during the 1993 summer have been documented. In terms of the coastal ocean, hypoxic conditions (oxygen concentrations below 2 $mg \cdot l^{-1}$) were elevated and more widespread than usual along the Louisiana coastline west of the delta (Rabalais et al., 1994). This can be attributed to two main causes. First, the high river discharges introduced abnormal amounts of nutrients during the summer months, fueling phytoplankton growth (Dortch, 1994). Second, the widespread low-salinity plume of river water was rapidly warmed by solar heating, resulting in a very stable water mass on the continental shelf. The increased phytoplankton biomass and the highly stratified water mass both exacerbated hypoxic conditions, which covered approximately double the area that would be expected in summer (Rabalais et al., 1994). The effects of hypoxic conditions on the productive Louisiana fishery has yet to be determined, however the widespread hypoxia in 1993 did have a negative impact on the benthic community west of the delta (Rabalais et al., 1994). The effects of increased river discharges east of the Mississippi delta are not known; however, hypoxia has not previously been found to be a problem in this area.

DISCUSSION

The relationship between the Mississippi River sediment plume and river discharge was investigated in year 1 of this project. In general, the size of the sediment plume was found to be a function of river discharge, higher discharge generally yielding larger plumes. The mean "composite" plume under low discharge conditions (0-10,000 $m^3 s^{-1}$) was observed to cover 1804 km^2 of the continental shelf. The mean "composite" plume under medium discharge conditions (10,001-20,000 $m^3 s^{-1}$) covered 2165 km^2 of the continental shelf. Under conditions of high river discharge (20,001-35,000 $m^3 s^{-1}$), the sediment plume covered 3909 km^2 (See Figure 4). The medium discharge plume was only 20% larger than the low discharge plume. However, the mean plume during periods of high river discharge was approximately double the size of the mean plume during medium discharge conditions.

In this study, the annual and interannual variability of the Mississippi River sediment plume was investigated. Annual plume variability was investigated by compositing satellite images during the month of October 1989 and during the March/April 1989 period. Minimum river discharge generally occurs from August through October and maximum discharge occurs from March through May. The 1989 year was fairly typical as during October 1989 discharge was low ($<$ 10,000 $m^3 s^{-1}$) and during the March/April period discharge was high, averaging 28,365 $m^3 s^{-1}$. The Mississippi sediment "composite" plume was 2058 km^2 in size during October 1989 and 4595 km^2 in March/April 1989. Similarly, an investigation of the interannual variability of the Mississippi plume during the spring of 4 years revealed that the average composite plume increased with increasing discharge. Thus, the time-averaged plume would be expected to vary both annually and interannually with large changes in river discharge.

The analysis of individual satellite images, however, revealed that the Mississippi River plume undergoes dramatic changes in areal extent and surface morphology on time scales as short as hours. Plume areas ranging in size from 822 km^2 to 7700 km^2 were observed from the satellite imagery obtained over the 5 year study period. A surprising result was that plume area could vary by as much as 3700 km^2 over a 24 hour period! Factors in addition to river discharge are, thus, controlling the day-to-day variability in plume morphology. There was evidence from the year 1 study that wind behavior was a key influencing factor to plume size. In this study, a detailed investigation of the effects of environmental variables on plume morphological parameters was made.

Results of the statistical analyses reveal that the size and morphology of the Mississippi River sediment plume is influenced by several environmental forcing factors. The most important factors determining plume area were found to be river discharge, wind components averaged over the 12 hours prior to image acquisition, and wind speed. Tidal phase and range explained very little of the variability in plume area or surface morphology. These results contrast with those obtained for the Mobile Bay plume (Abston et al, 1987; Dinnel et al., 1990) where tidal range and phase were more important in explaining plume area than the local winds.

The relationships between plume morphological parameters and environmental variables were were found to vary with season. Better correlations were obtained by separating the satellite imagery into "summer" and "winter" periods. The "summer" period included the months May through September and the "winter" period included the months October through April. During

"summer", a significant negative correlation was found between the western plume area and wind speed, indicating that largest plumes occur under low wind conditions, and vice versa. This interesting finding was further investigated by compositing the summer data according to wind direction. Linear regression techniques revealed that the observed negative relationship between wind speed and western plume area is strongest when wind forcing is eastward. An R^2 of 0.5 was obtained for the images preceded by eastward winds and an R^2 of 0.05 was obtained for the images preceded by westward winds. Thus, the negative correlation occurs during summer in association with eastward wind forcing.

It is hypothesized that the observed seasonal change in the sediment plume's response to wind speed in the western delta region may result from seasonal changes in upper-ocean stratification throughout the year. During late spring and summer, the low-density river water is heated rapidly at the surface by incoming solar radiation. This lowers the density of the fresh-water plume and increases the near-surface stratification of the water column. In the absence of wind, the plume undergoes buoyant spreading and the sediment is maintained at the surface by the shallow pycnocline. However, when the wind speed increases substantially, wind-waves increase vertical motion, reducing stratification, and the sediment is mixed downwards rather than spreading laterally. Research by Wright (1970) demonstrated that rough seas significantly increase the thickness of the plume south of the delta. Eastward wind forcing would subject the western plume area to considerable wind-wave mixing whereas westward wind forcing would not. The critical wind speed for initiation of vertical mixing appears to be about 5 m/s. Plumes less than 1500 km^2 in area were observed under moderate to strong eastward wind forcing (> 5 m/s). When eastward winds were less than 5 m/s plumes ranged from 2000 to 5500 km^2. In summary, these study results suggest that moderate to strong eastward winds induce vertical mixing of the plume west of the delta during summer which reduces the area of the surface sediment plume as observed by satellite.

Multiple regression techniques were employed in an attempt to use the relationships observed between the plume parameters and the environmental variables to help establish predictive models for the Mississippi River sediment plume's variability. Plume area was found to be more predictable than plume length. The best model was obtained for the eastern area of the plume from May through September when 70% of plume variability was explained by river discharge and local wind behavior. Plume area increased in size with increasing discharge and increasing frequency of northward and eastward winds. Winds blowing towards the east and northeast would induce water level set-up west of the delta which would inhibit flow out of the minor passes west of the delta and increase flow out of the eastern passes. In addition to the enhancement of flow east of the delta, northeastward winds would increase the eastward dispersal of surface suspended sediment through Ekman dynamics. Eastward winds should be less effective in dispersing the sediment since the east side would be in the lee of the wind. The largest sediment plumes east of the delta were observed after exposure to at least 12-hours of strong northeastward wind forcing (8 to 10 m s^{-1}) when river discharge was high. In predicting the eastern extent of the plume, local wind behavior was found to be more important than river discharge. The enormous sediment plume observed east of the delta on August 1993 (Figure 18), subsequent to the Great Flood of 1993, provides an excellent example of how efficiently the surface sediment is dispersed towards the east under prolonged exposure to northward and northeastward winds (Walker et al., 1994). In this extreme case, so much Mississippi River water flowed onto the continental shelf east of the delta that a detectable

amount reached the Florida Keys and the east coast of the United States, entrained by southward-flowing currents associated with the eastern edge of the Loop Current.

The second best predictive model was obtained for the western plume area during the summer months. In this case, 64% of the variability in plume area was explained by river discharge, wind speed, and the east-west wind component. The western plume area was maximized under conditions of high river discharge and weak eastward winds. During winter, the western plume area was maximized primarily by the presence of high river discharge and secondarily by strong southward and eastward winds. However, individual images demonstrated that some of the largest western plumes were observed under medium river discharge conditions, after prolonged exposure to strong southward winds associated with winter frontal passages. The predictive models for distance west were somewhat inferior to those for area west, however, the environmental variables included in the models were similar. The western extent of the plume was maximized by high river discharge and by southward winds. The best model was obtained during the summer months when river discharge, wind speed and the north-south wind component explained 54% of the variability in plume distance west of the delta.

The best predictive model for the offshore extent of the sediment plume was obtained with the summer data. The environmental factor of primary importance was the occurrence of eastward winds. River discharge was the second most important factor. Wind speed also affected plume morphology. The offshore dispersal of suspended sediments increased when eastward winds were relatively weak (<5 m/s). During the winter months, the presence of high river discharge and increased frequency/intensity of eastward winds explained most of the variability in the offshore dispersal of sediments. Thus, Ekman transport of shelf water occurs under conditions of eastward winds and the net result is a greater dispersal of river sediments into deeper waters seaward of the Balize delta. In most instances, the maximum seaward extent of river sediments occurred either south or southwest of the delta (See Figures 13 and 15).

This study has demonstrated the all-important role of wind forcing to the fate of river sediments from the Mississippi River delta in the northern Gulf of Mexico. In most cases, the plume's response to the wind was maximized after 12 hours. The morphology of the Mississippi River plume is more complicated than most river plumes as several passes are active and water flows into the Gulf of Mexico from the east, south, and west sides of the Balize delta. The five plume measurements, chosen to represent variability in plume morphology, demonstrated that the various plume areas are affected by winds from different directions. The eastern plume is maximized by northeastward winds. The western plume is maximized by eastward and southward winds. The offshore extent of the sediment plume is enhanced by eastward winds.

The model results, presented here, are surprisingly encouraging and demonstrate that the plume's areal extent and surface morphology are somewhat predictable from readily accessible environmental variables. These results have demonstrated some of the most important physical processes controlling morphological variations of the surface sediment plume as well as those controlling shelf circulation in the vicinity of the Mississippi River delta. One potentially important variable which was not easily incorporated into this study was information on shelf and slope currents at the time of image acquisition. South and east of the delta, currents may be particularly variable as a result of intrusions of the Loop Current or small eddies shed from the Loop Current (Wiseman and Dinnel 1988; Walker and Rouse 1993). Their presence could

have an additional influence on plume morphology. In year 1 of this study it was shown that the presence of Loop eddies seaward of the delta can enhance the offshore transport of river water and sediments.

CONCLUSIONS AND RECOMMENDATIONS

An analysis of satellite imagery over the time period 1989 to 1994 has enabled a quantitative investigation of the spatial and temporal variabilities of the sediment plume and the identification of important environmental forcing factors affecting plume dispersal.

The Mississippi River sediment plume (defined as suspended sediment concentrations > 10 $mg \cdot l^{-1}$) was found to range in size from 822 km^2 under low river discharge conditions to 7700 km^2 under high river discharge conditions. Although the time-averaged plume was associated with large changes in river discharge, substantial variability in plume area and morphology was observed which was unrelated to river discharge.

Correlation and multiple regression techniques were used to identify the most important environmental variables affecting plume variability and to quantify these relationships for possible predictive applications. Wind forcing was identified as the most important environmental variable, after river discharge. West of the delta, plume area was increased throughout the year by an increased frequency of eastward winds. During winter, southward and eastward winds increased plume area west of the delta. Southward winds were also associated with increases in the western extent of the sediment plume. Northward and eastward winds increased the size and extent of the plume east of the delta. The offshore southern extent of the plume was maximized by eastward winds. The use of wind data, averaged over the 12 hours prior to image acquisition, yielded the best correlation results. Tidal phase and range explained very little of the variability in plume area or length.

An interesting and surprising result was obtained for the western plume. The relationships between the western plume parameters and the environmental variables were found to change with the season. During summer under eastward wind conditions, wind speed was negatively correlated with plume area and length whereas during winter it was not. It is hypothesized that the observed seasonal change in the surface sediment plume's response to wind speed results from seasonal changes in upper ocean stratification. This hypothesis needs to be tested with field measurements west of the delta under appropriate wind conditions.

The plume parameters best predicted by the multiple regression models were plume area, east and west of the delta. The best predictive model for the western area was obtained from May through September when 64% of plume variability was explained by river discharge, wind speed, and the east-west wind component. The best model for the eastern plume area was obtained from May through September when river discharge, the north-south and east-west wind components explained 70% of plume variability. Thus, the model results have revealed that the plume's areal extent and surface morphology are somewhat predictable from readily accessible environmental variables.

This satellite study has enabled a summary of the circulation of Mississippi River water under various wind regimes. Throughout the year, the prevalence of westward winds ensures that a larger percentage of river water flows westward than eastward once discharged into the northern Gulf of Mexico. To the west of the delta, the surface circulation is generally anticyclonic (clockwise) within the Louisiana Bight, although a portion of the plume often continues flowing westward along the coast. Winds blowing towards the northeast, east and southeast can disrupt

the anticyclonic circulation and westward flow along the coast and efficiently force plume waters seaward, maximizing the offshore transport of river water and sediments. During periods of southwestward wind subsequent to winter frontal passages, the westward flow of river water and sediments from the east side of the delta may increase. Under the influence of strong southward and southwestward winds, river water from the eastern passes and ambient coastal waters are forced southward along the eastern side of the delta. They subsequently turn westward to join the discharge emanating from South Pass and Southwest Pass. During such episodes of southwestward wind forcing, almost all of the Mississippi River discharged into the Gulf of Mexico may be forced southwestward and westward along the Louisiana continental shelf and slope. During spring and summer when winds primarily blow towards the northwest, discharge from Southwest Pass and South Pass flow westward, whereas, discharges emanating from passes east of the delta flow into Chandeleur-Breton and Mississippi Sounds. Northward and northeastward winds enhance the eastward flow of river water. In an extreme case, during the Flood of Summer 1993, most of the river water and sediments moved eastward onto the Mississippi, Alabama, and Florida continental shelves and slopes for a period of several weeks.

The sole use of satellite imagery to define plume morphology may have resulted in an over-simplification of the Mississippi River plume. Future research on the plume's variability should include information on the sub-surface characteristics of the sediment plume. This may enable the identification of additional environmental variables or measurements which could further improve the predictive models presented here.

LITERATURE CITED

Abston, J., S. Dinnel, W. Schroeder, A. Shultz, and W. Wiseman, Jr. 1987. Coastal sediment plume morphology and its relationship to environmental forcing: Main Pass, Mobile Bay, Alabama. Coastal Sediments '87. WW Div/ASCE, New Orleans, LA. pp. 1989-2005.

Atkinson, L.P. and D. Wallace. 1975. The source of unusually low surface salinities in the Gulf Stream off Georgia. Deep-Sea Res. 23:913-916.

Chew, F., K.L. Drennan, and W.J. Demoran. 1962. Some results of drift bottle studies off the Mississippi Delta. Limnol. Oceanogr. 7:252-257.

Cochrane, J.D. and F.J. Kelley. 1986. Low-frequency circulation on the Texas-Louisiana continental shelf. Journal of Geophysical Research. 91(C9):10,645-10,659.

Dagg, M.J. and T.E. Whitledge. 1991. Concentrations of copepod nauplii associated with the nutrient rich plume of the Mississippi River. Continental Shelf Research. 11(11):1409-1423.

Dagg, M.J., P.B. Ortner, and F. Al-Yamani. 1987. Winter-time distribution and abundance of copepod nauplii in the northern Gulf of Mexico. Fishery Bulletin. 86:319-330.

Dinnel, S.P. and W.J. Wiseman, Jr. 1986. Fresh water on the Louisiana and Texas shelf. Continental Shelf Research. 6(6):765-784.

Dinnel, S.P., W.W. Schroeder, and W.J. Wiseman, Jr. 1990. Estuarine-shelf exchange using Landsat images of discharge plumes. Journal of Coastal Research. 6(4):789-799.

Dortch, Q. 1994. Changes in phytoplankton numbers and species composition. Coastal Oceanographic Effects of 1993 Mississippi River Flooding, Special NOAA Report, Ed. M.J. Dowgiallo, NOAA Coastal Ocean Office/National Weather Service. Silver Spring, MD. 76 pp.

Ebbesmeyer, C.C., G.N. Williams, R.C. Hamilton, C.E. Abbott, B.C. Collipp, and C.F. McFarlane. 1982. Strong persistent currents observed at depth off the Mississippi River delta. Proc 14th Int. Offshore Tech. Conf. Houston, TX. pp. 259-267.

Fernandez-Partegas, J. and C.N.K. Mooers. 1975. Some front characteristics over the eastern Gulf of Mexico and surrounding land areas. Final report to the Bureau of Land Management under contract 08550-CT4-L6.

Fisk, H.N., E. Mc Farlan, C.R. Kolb, and L.J. Wilbert. 1954. Sedimentary framework of the modern Mississippi delta. J. Sedimentary. V. 24.

Gagliardini, D.A., H. Karszenbaum, R. Legeckis, and V. Klemas. 1984. Application of Landsat MSS, NOAA/TIROS AVHRR, and Nimbus CZCS to study the La Plata River and its interaction with the ocean. Remote Sensing of Environment. 15:21-36.

Gilbert, P., T. Lee, G. Podesta, and P. Ortner. 1994. Mississippi River water in the Florida Straits. EOS, Trans., A. G. U. Ocean Science Meeting, Suppl, 75:209.

Huh, O.K. and K. J. Schaudt. 1990. Satellite imagery tracks currents in Gulf of Mexico. Oil and Gas Journal. 88(19):70-76.

Huh, O.K., W.J. Wiseman, Jr., and L.J. Rouse, Jr. 1978. Winter cycle of sea surface thermal patterns: Northeastern Gulf of Mexico. Journal of Geophysical Research. 83(C9):4523-4529.

Lee, T., G. Podesta, E. Williams, J. Splain, and J. Johnson. 1994. Low salinity water in the Straits of Florida. Coastal oceanographic Effects of 1993 Mississippi River Flooding, Special NOAA Report, Ed. M.J. Dowgiallo, NOAA Coastal Ocean Office/National Weather Service, Silver Spring, MD. 76 pp.

Lohrenz, S.E., M.J. Dagg, and T.E. Whitledge. 1990. Enhanced primary production at the plume/oceanic interface of the Mississippi River. Continental Shelf Research. 10(7):639-664.

McClain, E.P., W.G. Pichel, and C.C. Walton. 1985. Comparative performance of AVHRR-based multichannel sea surface temperatures. Journal of Geophysical Research. 90:11,587-11,601.

Milliman, J.D. and R.H. Meade. 1983. World-wide delivery of river sediment to the ocean. Journal of Geology. 91(1):1-21.

Mossa, J. 1990. Discharge-suspended sediment relationship in the Mississippi-Atchafalaya River system, Louisiana. Ph.D. Thesis. Louisiana State University. Baton Rouge, LA., 180 pp.

Muller-Karger F.E., C.R. McClain, and P.L. Richardson. 1988. The dispersal of the Amazon's water. Nature. 333:56-58.

Murray, S.P. 1972. Observations on wind, tidal and density-driven currents in the vicinity of the Mississippi River delta. In Shelf Sediment Transport. Eds. Swift. Duane and Pilkey. Dowden, Hutchinson and Ross, Inc. Stroudsburg, PA. 127-142.

Rabalais, N.N., R.E. Turner, and W.J. Wiseman. 1994. Hypoxic conditions in bottom waters on the Louisiana-Texas shelf. Coastal Oceanographic Effects of 1993 Mississippi River Flooding, Special NOAA Report, Ed. M.J. Dowgiallo, NOAA Coastal Ocean Office/National Weather Service, Silver Spring, MD. 76 pp.

Rabalais, N.N., R.E. Turner, W.J. Wiseman, Jr., and D.F. Boesch. 1991. A brief summary of hypoxia on the northern Gulf of Mexico continental shelf: 1985 - 1988. In: Tyson, R.V. and T.H. Pearson. Modern and Ancient Continental Shelf Anoxia. pp. 35-47.

Rhodes, R.C., A.J. Wallcraft, and J.D. Thompson. 1985. Navy-corrected geostrophic wind set for the Gulf of Mexico. NORDA Technical Note 310. 103 pp.

Richards, F. 1994. Hydrometeorological setting. Coastal Oceanographic Effects of 1993 Mississippi River Flooding, Special NOAA Report, Ed. M.J. Dowgiallo, NOAA Coastal Ocean Office/National Weather Service, Silver Spring, MD. 76 pp.

Rouse, L.J. and J.M. Coleman. 1976. Circulation observations in the Louisiana Bight using LANDSAT imagery. Remote Sensing of Environment. XL:635-642.

Schroeder, W.W., O.K. Huh, L.J. Rouse, Jr., and W.J. Wiseman, Jr. 1985. Satellite observations of the circulation east of the Mississippi Delta: Cold-air outbreak conditions. Remote Sensing of Environment. 18:49-58.

Schroeder, W.W., S.P. Dinnel, W.J. Wiseman, Jr., and W.J. Merrell, Jr. 1987. Circulation patterns inferred from the movement of detached buoys in the eastern Gulf of Mexico. Continental Shelf Research. 7:883-894.

Smith, N.P. 1980. On the hydrography of shelf waters off the central Texas gulf coast. Journal of Physical Oceanography. 10:806-813.

Sogard, S.M., D.E. Hoss, and J.J. Govoni. 1987. Density and depth distribution of larval Gulf menhaden, Brevoortia patronus, Atlantic croaker, Micropogonias undulatus, and spot, Leiostomus xanthurus, in the northern Gulf of Mexico. Fishery Bulletin. 85:601-609.

Stumpf, R.P. 1988. Remote sensing of suspended sediments in estuaries using atmospheric and compositional corrections to AVHRR data. Proceedings of the 21st Intl. Symp. on Remote Sensing of Environment. Ann Arbor, MI. pp. 205-222.

Stumpf, R.P. 1992. Remote sensing of water quality in coastal waters. Proceedings of the First Thematic Conference on Remote Sensing for Marine and Coastal Environments. New Orleans, LA. 15-17 June 1992. SPIE 1930:293-305.

Tester, P. and L. Atkinson. 1994. Low salinity water in the Gulf stream off North Carolina. Coastal Effects of 1993 Mississippi River Flooding, Special NOAA Report, Ed. M.J. Dowgiallo, NOAA Coastal Ocean Office/National Weather Service, Silver Spring, MD. 76 pp.

U.S. Army Corps of Engineers. 1984. Mississippi River, Baton Rouge to the Gulf Louisiana Project. Final Environmental Impact Statement Supplement II. Appendix E. pp. E-9.

Walker, N.D., G. Fargion, L.J. Rouse, and D. Biggs. 1994. Circulation of Mississippi River water discharged into the northern Gulf of Mexico by the Great Flood of Summer 1993. EOS, Transactions, American Geophysical Union, V.75 no.36.

Walker, N.D. and L.J. Rouse. 1993. Satellite assessment of Mississippi River discharge plume variability. U.S. Department of the Interior, Minerals Management Service, Gulf of Mexico OCS Region, New Orleans, LA., OCS Study MMS 93-0044. 50 pp.

Walsh, J.J., D.A. Dieterle, M.B. Meyers, and F.E. Muller-Karger. 1989. Nitrogen exchange at the continental margin: A numerical study of the Gulf of Mexico. Progress in Oceanography. 23:245-301.

Wiseman, W.J., Jr. and S.P. Dinnel. 1988. Shelf currents near the mouth of the Mississippi River. Journal of Physical Oceanography. 18:1287-1291.

Wiseman, W.J., Jr., J.M. Bane, S.P. Murray, and M.W. Tubman. 1976. Small-scale temperature and salinity structure over the inner shelf west of the Mississippi River delta. Memoires Societe Royale des Sciences de Liege. 6e serie. tome X. pp. 277-285.

Wright, L.D. 1970. Circulation, effluent diffusion, and sediment transport, mouth of South Pass, Mississippi River delta. Coastal Studies Institute Technical Report. No. 84. Baton Rouge, LA. 60 pp.

Wright, L.D. and J.M. Coleman. 1971. Effluent expansion and interfacial mixing in the presence of a salt wedge, Mississippi River Delta. Journal of Geophysical Research. 76:8649-8661.

Wright, L.D. and J.M. Coleman. 1974. Mississippi River mouth processes: effluent dynamics and morphologic development. Journal of Geology. 82:751-778.

The Department of the Interior Mission

As the Nation's principal conservation agency, the Department of the Interior has responsibility for most of our nationally owned public lands and natural resources. This includes fostering sound use of our land and water resources; protecting our fish, wildlife, and biological diversity; preserving the environmental and cultural values of our national parks and historical places; and providing for the enjoyment of life through outdoor recreation. The Department assesses our energy and mineral resources and works to ensure that their development is in the best interests of all our people by encouraging stewardship and citizen participation in their care. The Department also has a major responsibility for American Indian reservation communities and for people who live in island territories under U.S. administration.

The Minerals Management Service Mission

As a bureau of the Department of the Interior, the Minerals Management Service's (MMS) primary responsibilities are to manage the mineral resources located on the Nation's Outer Continental Shelf (OCS), collect revenue from the Federal OCS and onshore Federal and Indian lands, and distribute those revenues.

Moreover, in working to meet its responsibilities, the **Offshore Minerals Management Program** administers the OCS competitive leasing program and oversees the safe and environmentally sound exploration and production of our Nation's offshore natural gas, oil and other mineral resources. The MMS **Minerals Revenue Management** meets its responsibilities by ensuring the efficient, timely and accurate collection and disbursement of revenue from mineral leasing and production due to Indian tribes and allottees, States and the U.S. Treasury.

The MMS strives to fulfill its responsibilities through the general guiding principles of: (1) being responsive to the public's concerns and interests by maintaining a dialogue with all potentially affected parties and (2) carrying out its programs with an emphasis on working to enhance the quality of life for all Americans by lending MMS assistance and expertise to economic development and environmental protection.